Phosphorus limitation affects the molecular composition of Thalassiosira weissflogii leading to increased biogenic silica dissolution and high degradation rates of cellular carbohydrates

Christos Panagiotopoulos, Madeleine Goutx, Maxime Suroy, Brivaëla Moriceau

Phosphorus limitation affects the molecular composition of *Thalassiosira weissflogii* leading to increased biogenic silica dissolution and high degradation rates of cellular carbohydrates

Christos Panagiotopoulos[1*], Madeleine Goutx[1], Maxime Suroy[1], Brivaela Moriceau[2]

[1]*Aix Marseille Univ., Université de Toulon, CNRS, IRD, Mediterranean Institute of Oceanography (MIO) UM 110, 13288, Marseille, France*

[2]*Université de Brest, Institut Universitaire Européen de la Mer (IUEM), CNRS, Laboratoire des Sciences de l'Environnement Marin, UMR 6539 CNRS/UBO/IFREMER/IRD, 29280 Plouzané, France*

Corresponding author e-mail: christos.panagiotopoulos@mio.osupytheas.fr

Abstract

Diatoms in general, and *Thalassiosira weissflogii* (*T. weissflogii*) in particular, are among the most ubiquitous phytoplanktonic species while, phosphorus (P) is an essential nutrient that limits productivity in many oceanic regimes. To investigate how *T. weissflogii* cultures grown under different P regimes are chemically altered before and during their prokaryotic degradation, *T. weissflogii* cells were cultivated under two contrasting P conditions, “P-stress” and “P-replete”. Biodegradation experiments were conducted in natural seawater comprising a natural prokaryotic community. The particulate fraction was monitored for 3 weeks for organic carbon (POC), nitrogen (PON), biogenic silica ($bSiO_2$), total carbohydrates (PCHO) and individual monosaccharides, including prokaryotic counting. Our results indicated that P-stress induced changes in the chemical composition of the *T. weissflogii* cells, causing a decrease to the Si/N (1.1 to 0.46) and Si/C (0.17 to 0.08) ratios. The “P-stress *T. weissflogii*” cells were characterized by high amounts of galactose (23% of PCHO), xylose (21%), and glucose (19%) compared to the “P-replete *T. weissflogii*” cells, which were dominated by ribose (20% of PCHO), further indicating the exhaustion of ribose-rich molecules (e.g., ATP) in *T. weissflogii* under “P-stress” conditions. The degradation experiments showed that $bSiO_2$ produced under “P-stress” conditions dissolved more rapidly than $bSiO_2$ formed under “P-replete” conditions, whereas POC and PON exhibited higher degradation rate constants in the “P-replete *T. weissflogii*” than in the “P-stress *T. weissflogii*” experiment. Overall, these observations show that T. *weissflogii* submitted to P-limitation, results in changes in its initial biochemical composition, increases frustule dissolution rate, and decreases the degradation of *T. weissflogii*-organic matter by marine prokaryotes.

Keywords: Bacterial biodegradation, *Thalassiosira weissflogii*, P-stress, POC, PON, carbohydrates, biogenic silica.

1. Introduction

Nitrogen (N) and phosphorus (P) are among the most important nutrients in terrestrial and aquatic ecosystems. The former is mainly involved in the production of plant and animal tissues (protein synthesis), whereas the latter is fundamental in many biological processes as well as in structural components of cells (e.g., RNA and DNA, energy transactions via ATP; Lehninger et al., 1993; Berg et al., 2002; Karl and Björkman, 2015). Although N and P belong to the same group of elements on the periodic table and they both contribute to eutrophication phenomena (i.e., act as fertilizers; Ryther and Dunstan, 1971; Gruber and Galloway, 2008; Némery and Garnier, 2016), they exhibit different oxidation states, have different uptake pathways (e.g., N can be retrieved from the atmosphere by diazotrophs), and their N/P ratio may span from < 16 to > 100 (Vitousek and Howarth, 1991; Downing, 1997; Paytan and McLaughlin, 2007; Godwin and Cotner, 2015; Karl and Björkman, 2015). Although the N and P cycles are closely linked to one another, P appears to be more critical as a limiting element (Trommer et al., 2013). This is not only because of its low proportions compared to N, but also because it cannot be found in the atmosphere in a gaseous state (Paytan and McLaughlin, 2007; Karl and Björkman, 2015). Therefore, the availability of P is critical for cell growth in marine ecosystems, especially for phytoplankton (Redfield et al., 1963; Jackson and Williams, 1985; Thingstad et al., 2005; Paytan and McLaughlin, 2007).

Despite the fact that P sources in seawater are numerous, whether in inorganic or organic forms (Karl and Björkman, 2015), phytoplanktonic organisms very often cannot grow and eventually turn over as a result of P-stress. P-stress conditions have been observed in different parts of the ocean, including the China Sea (Harrison et al., 1990a), the northwestern Mediterranean Sea (Thingstad et al., 2005), and the western North Atlantic Ocean (Wu et al., 2000). Several studies have assessed the impact of P-starvation stress in phytoplankton in terms of cellular growth; P-competition with other species, including bacteria; the extracellular release of organic compounds; and the biosynthesis of intracellular organic compounds (Urbani et al., 2005; Zohary et al., 2005; Moore et al., 2008; Tanaka et al., 2011; Sebastian et al., 2016). Furthermore, other studies showed that the phytoplankton in the ocean uses non-phosphorus lipids in response to P scarcity stress (Van Mooy et al., 2009; Obata et al., 2013; Brembu et al., 2017). All these studies show the importance of P on structuring the ocean phytoplankton community and on the metabolism of microalgae cells. Despite this wealth of information on P-stress on phytoplankton species, the subsequent degradation of phytoplankton grown under P-stress is a research topic that has not been thoroughly examined until now in the scientific literature. Thus, despite the fact that several studies have focused on the degradation of phytoplankton and sinking marine particles by following their bulk individual components (e.g., proteins, carbohydrates, lipids, etc.; Harvey et al., 1995; Harvey and Macko, 1997; Panagiotopoulos et al., 2002; Goutx et al., 2007; Engel et al., 2009) for 2-3 weeks, very little is known on the chemical alteration of frustules, including the silica dissolution and decomposition rates of P-stress grown diatoms that further impact the export of photosynthetic carbon. Indeed, biogeochemical models predict a future increase in nutrient limitation across most of the

ocean (Bopp et al., 2005). Consequently, it is important to study whether P-stress grown diatoms have the potential to be rapidly mineralized or accumulated within the dissolved organic matter pool or marine sediments, which further determines the time scale at which mineralized diatom carbon will reach the atmosphere.

The present study aims to examine the prokaryotic degradation and the frustule dissolution, and thus, the fate of marine diatoms that are previously grown under different P-conditions ("P-replete" and "P-stress"). In this study we followed the changes in the chemical composition of a very well-known diatom species, *Thalassiosira weissflogii*, by monitoring particulate organic carbon (POC), organic nitrogen (PON), biogenic silica ($bSiO_2$), and total carbohydrates (PCHO) over a period of 3 weeks. In contrast to previous investigations that estimated degradation rates on 3-day to 1-week experiments (Goutx et al., 2007; Wetz et al., 2008; Piontek et al., 2009), we chose this unusual long-term degradation experiment recognizing that dead diatoms may reside for a long period of time in the ocean and especially in the bathypelagic layers (Agusti et al., 2015). It is important to note that a 3-week degradation experiment requires that the starting conditions must contain a high amount of diatom cells in order to follow their different pools (i.e., POC, PON, PCHO, and $bSiO_2$), which is only feasible using a dense diatom culture (Sun et al., 1993; Suroy et al., 2015). At the molecular level, the effect of P-stress on the degradation rate constants of the individual monosaccharides was also evaluated. The results are compared and discussed along with the bulk degradation features of the POC, PON, $bSiO_2$ and PCHO.

2. Materials and Methods

2.1. Experimental design

The experimental protocol used in this study has been set up to follow the impact of P-stress on the degradation of the different pools of organic and inorganic matter (POC, PON, and $bSiO_2$), including the PCHO in dead diatoms, for 3 weeks. We used *T. weissflogii* as a model diatom as this ubiquitous species has extensively been studied in terms of transparent polymer production (Chen et al., 2015), aggregation and sedimentation (Seebah et al., 2014), growth rates under N- and Si- starvation (De La Rocha et al., 2010; Suroy et al., 2015), and photosynthetic efficiency under P-stress (Liu et al., 2011). A schematic view of the experimental protocol employed in this study is presented in Fig. 1. Briefly, *T. weissflogii* cells were grown under two different conditions, namely, "P-replete *T. weissflogii*" (control condition) and "P-stress *T. weissflogii*". *Thalassiosira weissflogii* cells were then killed and inoculated in 0.7 µm filtered seawater containing its natural prokaryotic community, to monitor the net degradation for 3 weeks.

2.1.1. Preparation of "P-replete" and "P-stress" T. weissflogii *cultures*

The marine ubiquitous diatom *T. weissflogii* (strain CCMP 1049) was obtained from the IFREMER facility (Argenton station, France), and the initial culture in f/2 medium was treated with a mix of antibiotics, including penicillin G, streptomycin, and gentamycin, to remove bacteria (Guillard, 2005). The absence of bacteria was checked by placing the inoculum on ZoBell agar plates (ZoBell, 1941). The PO_4^{3-} starvation experiments were undertaken in a 10 L batch culture by switching the medium supply from normal f/2 to a PO_4^{3-}-free f/2 medium (Guillard and Ryther, 1962; Fig. 1). As such, two 10 L culture batches were prepared: one "P-stress *T. weissflogii*" batch and one "P-replete *T. weissflogii*" batch. Both axenic cultures in batches were maintained

151 for 1 week at 18 °C (± 1 °C) under a light/dark cycle (16 h: 8 h) under a photon flux
152 density of 180 µmol photons m^{-2} s^{-1}. The impact of P-stress on *T. weissflogii* cells was
153 evaluated by monitoring the photosynthetic parameters using fluorescence (WATER/B
154 – PAM, Walz, Effeltrich, Germany; Schreiber et al., 1986) and Fourier-transform
155 infrared spectroscopy (Tensor 27 BRUKER; Beardall et al., 2001). The maximum
156 energy conversion efficiency or quantum efficiency of photosystem II charge separation
157 (Fv/Fm) decreased from 0.6 to 0.3 on day 7. At this time, the maximum photosynthetic
158 electron transport rate (ETR_{max}) obtained from light curves relating the ETR to the
159 irradiance decreased from 2.9 to 0.013, indicating that "P-stress *T. weissflogii*" cells
160 were not able to maintain photosynthesis after 7 days (Soler, 2010). The FTIR spectra
161 of the entire cells also showed significant changes in the *T. weissflogii* cell structure
162 under P-stress conditions (Fig. S1). The *T. weissflogii* cell numbers obtained in the 10 L
163 batches after this treatment were approximately 1.8 x 10^8 cell L^{-1} for both cultures ("P-
164 replete *T. weissflogii*" and "P-stress *T. weissflogii*"). The *T. weissflogii* cultures were
165 then concentrated by centrifugation (20 min at 2000 rpm), the supernatant was
166 discarded, and the pellets were frozen at –80 °C for 24 h to kill *T. weissflogii* without
167 breaking their cells (Soler, 2010; Fig. 1).
168
169 *2.1.2. Degradation experiment*
170 The pellets of the *T. weissflogii* cells grown in the two different treatments ("P-
171 replete" and "P-stress") were resuspended in 12 L degradation batches that were filled
172 with 0.7 µm filtered natural seawater sampled at a depth of 10 m in the Bay of Brest.
173 The final *T. weissflogii* cell concentration was similar in the two degradation batches
174 (Table 1) and large enough to ensure a clear signal for all the measured parameters until

the end of the 3 week degradation experiment (see below). The nitrate, phosphate, and silicate concentrations in seawater on the day of sampling were 0.33, 0.05, and 0.66 µM, respectively. The seawater temperature was 15.8 °C, which was almost identical to that used for the incubation experiments (see below). The seawater was filtered at 0.7 µm GF/F (47 mm, Whatman; baked at 450 °C for 6 h) to remove phyto- and zooplanktonic organisms while maintaining most of the natural prokaryotic community (Duhamel et al., 2007; Suroy et al., 2015).

The prokaryotic inoculum concentrations were estimated before the addition of *T. weissflogii*. *Thalassiosira weissflogii* cellular concentrations were estimated on day 1, considering that 24 h are necessary for *T. weissflogii* cells to adapt to the new medium (prokaryotes plus dead *T. weissflogii* cells), resulting in a homogenous mixture for sampling. Hence, we considered that the degradation experiment started 24 h after the setup of the degradation batches, assuming that there was little variability in the POC, PON, $bSiO_2$, and PCHO concentrations between day 0 and day 1 of the experiment. Thus, the ratio of these parameters to the *T. weissflogii* cells did not change dramatically in this time interval. The degradation batches were placed on an orbital shaker table at 16 °C in the dark, and punched caps were used to ensure gas exchange. The batches were sampled daily for their biochemical parameters (POC, PON, $bSiO_2$, and PCHO), including the total counts of heterotrophic prokaryotes over 21 days. Replicate samples (n = 2–3) were taken throughout the degradation experiments, mainly on days 2, 6, 9, 12, and 19, depending on the experiment (see also figure captions). Prior to each sampling, the batches were gently shaken to ensure homogeneity. At the end of the experiment, approximately 40% of the initial volume remained in the bottle to minimize batch effects.

199 *2.2. Prokaryotic and T. weissflogii cell counts*

200 Prokaryotes were counted on 5 mL samples at each time point by flow
201 cytometry using a FacsVerse flow cytometer (Becton Dickinson, San Jose, USA). Data
202 from the flow cytometer were processed using the BD FacSuite^{Tm} software, according
203 to previously described methods (Troussellier et al., 1993; Marie et al., 1997; Marie and
204 Partensky, 2006). The *T. weissflogii* cell numbers were also measured by flow
205 cytometry on the first day of the biodegradation experiment to obtain information about
206 the initial *T. weissflogii* concentrations.

207

208 *2.3. POC and PON analysis*

209 Each day, a 10 mL sample from each of the degradation batches ("P-replete" and
210 "P-stress") was collected and filtered on 0.7 µm precombusted GF/F filters (450 °C, 6
211 h) for POC and PON concentration measurements. The filters were dried overnight in
212 an oven at 50 °C. The POC and PON levels were measured on the same filter using a
213 Carlo Erba NA 2100 CN analyzer coupled with a Finnigan Delta S mass spectrometer
214 (Nieuwenhuize et al., 1994). The detection limits were 5 µg and 1 µg for POC and
215 PON, respectively, with a standard error of 2–3%.

216

217 *2.4. SiO_2 analysis*

218 To monitor the $bSiO_2$ dissolution, each day 10 mL samples from each of the
219 degradation batches were filtered on 0.45 µm polycarbonate filters. Filtrates were
220 directly analyzed for dissolved silica (dSi; see below), whereas filters were dried
221 overnight and used for $bSiO_2$ analysis using a variation of the method of Ragueneau and
222 Tréguer (1994). Following this protocol, the filters were digested in 0.2 N NaOH during

4 h at 95 °C, then the solutions were cooled in ice, neutralized using 1 N HCl, and centrifuged to remove remaining solids. As no lithogenic silica was present in the algal culture, the second digestion step using HF was omitted. The overlying water was analyzed for dSi using the molybdate blue spectrophotometric method adapted by Gordon et al. (1993) for use in segmented flow colorimetry. Standards were made in distilled water for $bSiO_2$ analysis and artificial seawater for dSi. The analysis was performed on a Bran and Luebbe Technicon Autoanalyzer (< 1% precision).

2.5. PCHO analysis

Similar to the POC, PON, and $bSiO_2$ measurements, a 10 mL sample from each of the degradation batches was collected and filtered on 0.7 µm pre-combusted GF/F filters (450 °C, 6 h) for the PCHO analysis using the procedure described by Suroy et al. (2015). Briefly, filters were cut with clean scissors, transferred into glass tubes, and hydrolyzed with 1.2 M H_2SO_4 for 3 h at 100 °C (Panagiotopoulos and Wurl, 2009). The samples were neutralized with pre-combusted $CaCO_3$ (450 °C for 6 h) and were pipetted into scintillation vials for liquid chromatography analysis (Suroy et al., 2015).

A Dionex ICS-3000 anion exchange chromatograph fitted with a pulsed amperometric detector (HPAEC-PAD) was used for all PCHO analyses. Details of the analytical procedure have been provided elsewhere (Panagiotopoulos et al., 2012; Suroy et al., 2015). Ten individual monosaccharides were detected in the hydrolysates of the particulate organic material, including deoxysugars (fucose and rhamnose), pentoses (arabinose, ribose, and xylose), one amino sugar (glucosamine), hexoses (galactose, glucose, and mannose), and one acidic sugar (galacturonic acid). The neutral and amino sugars were separated with an isocratic 19 mM NaOH elution at 17 °C, whereas

galacturonic acid was detected in a separate analysis using a gradient elution (Panagiotopoulos et al., 2012). The flow rate was set at 0.7 mL min^{-1} for neutral and acidic sugar analyses. The data acquisition and processing procedures were performed using the software Chromeleon®. The analytical errors calculated by the coefficients of variation of the repeated injections of a standard solution of 50 nM/sugar were 5–10% and 0.9–2.0% (n = 6) for the peak area and retention time, respectively. The total particulate carbohydrate concentrations (µM) are given in C-equivalents and the relative abundances (mol%) of their monomeric constituents (e.g., monosaccharides) are given in Table 2.

2.6. Statistical analysis and estimation of kinetic parameters

The degradation of bulk organic matter (POC and PON), $bSiO_2$ dissolution, PCHO, and individual monosaccharides were monitored using a statistical comparison of three mechanistic models.

Model 1 is a simple first-order exponential rate equation (1) as described by Greenwood et al. (2001), that has been used in many dissolution/degradation studies (e.g., Kamatani and Riley, 1979; Kamatani et al., 1980; Kamatani, 1982):

$$\hat{C}_{(t)} = C_0.e^{(-k.t)} \quad (1)$$

where:

$\hat{C}t$ is the concentration (µM) estimated at time t (d),

C_0 is the initial concentration, and

k is the dissolution/degradation rate constant (d^{-1}).

Model 2 is a second-order equation (2) that considers two pools of organic matter with different reactivities. It is similar to the equation that was used by Westrich

and Berner (1984) for carbon degradation, and more recently it has also been employed for $bSiO_2$ dissolution (Moriceau et al., 2009; Boutorh et al., 2016):

$$\hat{C}_{(t)} = C_1.e^{(-k_1.t)} + C_2.e^{(-k_2.t)} \quad (2a)$$

where:

$\hat{C}t$ is the concentration (µM) estimated at time t (d),

C_1 and C_2 are the initial concentrations (µM) of pools 1 and 2, respectively, and

k_1 and k_2 are their respective degradation rate constants (d^{-1}).

As equation (2) uses more parameters, Model 2 always produces a better fit than Model 1. It was found that for most of the examined parameters (i.e., POC, PON, and PCHO), the second degradation rate constant (i.e., k_2) was equal to zero. In this case, the model only has 3 variables: C_1, C_2, and k_1 (see equation 2b).

$$\hat{C}_{(t)} = C_1.e^{(-k_1.t)} + C_2 \quad (2b)$$

The best model was chosen using the Shapiro-Wilk and Constant Variance Test statistical tests in Sigmaplot, which favors the goodness of fit and the lowest number of parameters. Likewise, the bulk parameters (POC and PON) and PCHO were best modeled using equation (2b), whereas individual monosaccharides and $bSiO_2$ were best modeled using equations (1) and/or 2(b) (Tables 3, 4).

3. Results

3.1. Initial observations

At the beginning of the biodegradation experiment, the diatom cell concentrations were 6.60 x 10^7 cell L^{-1} in the "P-replete *T. weissflogii*" degradation batch and 6.80 x 10^7 cells L^{-1} in the "P-stress *T. weissflogii*" degradation batch (Table

1). These concentrations are similar to those observed during a simulated *T. weissflogii* bloom (Diekmann et al., 2009) but an order of magnitude higher than those generally observed in "natural" bloom concentrations (Grattepanche et al., 2011; Smetacek, 1985).

The results indicated that the "P-stress *T. weissflogii*" growth conditions induced increases of 29% (mol %) in the carbon and 44% (mol%) in nitrogen per cell compared to the "P-replete *T. weissflogii*" conditions. On the other hand, $bSiO_2$ showed the opposite trend as it was lower in the "P-stress *T. weissflogii*" degradation batches than in the "P-replete *T. weissflogii*" degradation batches (Table 1).

In this study, POC and PON values (Table 1) were not corrected for prokaryotic carbon and nitrogen because only free and not attached prokaryotes were counted. Nevertheless, the POC and PON values presented here fall within the same order of magnitude as those generally reported for *T. weissflogii* species (Waite et al., 1992; De La Rocha et al., 2010) and agree well with the results of a previous study of the same species in which corrections for prokaryotic carbon and nitrogen were made (Suroy et al., 2015).

Prokaryotic concentrations were measured after 24 h in both the "P-replete *T. weissflogii*" and "P-stress *T. weissflogii*" degradation batches. The results showed that the prokaryotic concentrations were similar (5.6 and 7.0 x 10^{10} cell L^{-1}) for the "P-stress *T. weissflogii*" and "P-replete *T. weissflogii*" batches at the beginning of the experiments and that they peaked on day 1 (Table 1; Fig. 2). After day 1, prokaryotic concentrations slowly decreased to reach their first plateau on day 5 (2.5 and 3.1 x 10^{10} cell L^{-1} for the "P-stress *T. weissflogii*" and "P-replete *T. weissflogii*" batches, respectively) and a second plateau on day 12 (3.3 and 3.7 x 10^{10} cell L^{-1} for the "P-

stress *T. weissflogii*" and "P-replete *T. weissflogii*" batches, respectively) until the end of the experiment (Fig. 2). Such prokaryotic features observed during biodegradation experiments agree with previous results performed in sinking marine particles (Panagiotopoulos et al., 2002; Panagiotopoulos and Sempéré, 2007), *Skeletonema marinoi* (Moriceau et al., 2009), *Emiliania huxleyi* calcium carbonate frustule (Engel et al., 2009), and Si/N- stress *T. weissflogii* (Suroy et al., 2015), indicating that the decrease in the particulate organic matter pool is the result of prokaryotic respiration and growth.

The results of the degradation experiment in the "P-replete *T. weissflogii*" batch show increases in POC and PON concentrations (of approximately 50% and 60% for POC and PON, respectively), which were observed between T_0 and T_2 (Fig. 3). A similar pattern has already been observed in other studies and is probably due to re-aggregation of the < 0.7µm pool related to the addition of the prokaryotic community, which boosts the stickiness of the exopolymeric compounds (EPS) excreted by the *T. weissflogii* (Gärdes et al., 2010) as well as the heterogeneity in the batch (Suroy et al., 2015). In addition, PCHO, glucose, and galactose, which are known to be the main constituent of the EPS copiously secreted by diatoms (Magaletti et al. 2004; Urbani et al. 2005), also increased between T_0 and T_2 in the "P-replete *T. weissflogii*" batches, which further reinforces the hypothesis of re-aggregation (Fig. 4b; Fig.5). After T_2, the POC and PON concentrations decreased over time, which typically reflected the decomposition patterns of *T. weissflogii*-POC and *T. weissflogii*-PON (Fig. 3). In contrast to the "P-replete *T. weissflogii*" batch, the POC and PON concentrations in the "P-stress *T. weissflogii*" batch began to decrease at T_0.

342 Contrarily, as minute or no $bSiO_2$ is associated with the organic matter that re-
343 aggregates in the colloidal pool, the $bSiO_2$ concentrations remained rather stable in the
344 "P-replete *T. weissflogii*" batch during the first days of the experiment (Fig. 4a). Similar
345 to POC and PON, $bSiO_2$ concentrations also began to decrease at T_0 in the "P-stress *T.*
346 *weissflogii*" batch (Fig. 4a). The degradation of all the biochemical compounds is
347 expressed in our study as its decrease relative to its highest concentration measured
348 before the degradation/dissolution started.
349 Similar to POC, the initial concentration of the PCHO–C in the "P-stress *T.*
350 *weissflogii*" degradation batch was higher than in the "P-replete *T. weissflogii*"
351 degradation experiment (169 *vs.* 110 µMC; Table 2). At T_0, PCHO represented 14 and
352 16% of POC for the "P-replete *T. weissflogii*" and "P-stress *T. weissflogii*" degradation
353 experiments, respectively, indicating the slight preferential allocation of photosynthetic
354 carbon into *T. weissflogii* cells under "P-stress" conditions (Table 2). As for POC and
355 PON, the PCHO–C concentrations also peaked at T_2 (Fig. 4b) for the "P-replete *T.*
356 *weissflogii*" experiment, supporting the previously mentioned hypothesis regarding
357 DOM aggregation.
358 Qualitatively, the sugar composition recorded in *T. weissflogii* comprised three
359 aldohexoses, three aldopentoses, two deoxysugars, one aminosugar, and one uronic acid
360 (see above; Table 2). Five monosaccharides generally dominated the *T. weissflogii*
361 carbohydrate composition namely, galactose, glucose, xylose, ribose, and mannose.
362 These monosaccharides accounted for 65% and 78% of PCHO in the "P-replete *T.*
363 *weissflogii*" and "P-stress *T. weissflogii*" degradation batches, respectively, at the
364 beginning of the biodegradation experiment. It is worth noting that the "P-replete" batch

365 was particularly enriched with ribose (~20%) and galacturonic acid (2%) when
366 compared to the “P-stress” batch (Table 2).
367
368 *3.2. Organic matter degradation*
369 *3.2.1. Bulk parameters (POC, PON, and $bSiO_2$)*
370 The POC and PON degradation followed similar patterns in both batches, with
371 an initial period of degradation (approximately 7–8 days from the beginning of the
372 experiment) in which the *T. weissflogii*-organic matter degraded faster, followed by a
373 second period in which the *T. weissflogii*-organic matter concentrations remained
374 constant (Fig. 3a). The best fits for the degradation of the POC and PON were obtained
375 using equation 2b.
376 The k_1 degradation rate constant of POC was two times higher in the “P-replete
377 *T. weissflogii*” batch than in the “P-stress *T. weissflogii*” batch (0.40 ± 0.05 d^{-1} vs. 0.19
378 $\pm$ 0.05 d^{-1}; Table 4). The results showed that after 7–8 days of degradation,
379 approximately 36% of the POC from the “P-replete” experiment was decomposed,
380 whereas this amount was slightly higher for the “P-stress” experiment (approximately
381 43%) over the same period (Fig. 3a). Then, POC concentrations remained stable and
382 reached a plateau accounting for approximately 60% of the initial POC in both batches
383 (Fig. 3a).
384 The degradation rate constant of PON was higher in the “P-replete” batch than in
385 the “P-stress” batch (0.27 ± 0.02 d^{-1} vs. 0.17 ± 0.03 d^{-1}; Table 3). Similar to POC, after
386 7–8 days of degradation, PON concentrations reached a plateau that accounted for
387 approximately 40% of the initial PON in both batches (Fig. 3b). The $bSiO_2$ in the “P-
388 replete” and “P-stress” batches dissolved with the exponential decrease commonly

389 observed in dissolution experiments and $bSiO_2$ dissolution rate constants were
390 calculated according to model 1. An opposite trend was observed when compared to
391 POC and PON degradation, with a faster $bSiO_2$ dissolution in the "P-stress *T.*
392 *weissflogii*" batches than in the "P-replete *T. weissflogii*" batches. Frustules from the
393 "P-stress" *T. weissflogii* batch were dissolved with a rate constant of 0.05 ± 0.02 d^{-1},
394 about twice the rate calculated in the "P-replete *T. weissflogii*" batch (0.02 ± 0.01 d^{-1};
395 Table 3). After 3 weeks of dissolution, about 38% of the $bSiO_2$ has been dissolved in
396 the "P-replete *T. weissflogii*" batch while 64% of the $bSiO_2$ has been dissolved in the
397 "P-stress *T. weissflogii*" batch.
398
399 *3.2.2. PCHO*

400 In contrast to POC and PON, and alike $bSiO_2$, the degradation rate constant for
401 the PCHO–C was higher in the "P-stress *T. weissflogii*" batch (0.92 ± 0.18 d^{-1}) than in
402 the "P-replete *T. weissflogii*" batch (0.15 ± 0.08 d^{-1}), indicating a rapid degradation of
403 carbohydrates from *T. weissflogii* grown under P-stress conditions (Fig. 4b; Table 3). At
404 the end of 20 days of degradation, approximately 60% of the initial PCHO–C pool
405 remained in the "P-replete *T. weissflogii*" batch, whereas PCHO–C represented 30% of
406 the initial PCHO–C pool in the "P-stress *T. weissflogii*" batch.
407 The degradation rate constants showed significant differences between the
408 monosaccharides in these two experiments. In general, higher values were recorded in
409 the "P–stress" experiment than in the "P-replete" experiment, which agrees with the
410 pattern that was observed for the total PCHO pool (Table 3). Xylose, followed by
411 glucose and galactose, were the monosaccharides that exhibited the highest degradation
412 rates in the "P-stress" experiment (k_1 = 0.80–1.52 d^{-1}), whereas galacturonic acid,

ribose, and galactose rates reached the highest values in the "P-replete" experiment (k_1 = 0.17–0.49 d^{-1}; Fig. 5). The degradation rate constants of the other monosaccharides showed little (e.g., glucosamine and rhamnose) to no degradation (e.g., arabinose) in both experiments (Table 4). The non-degradable pool (i.e., C_2) comprised 29–83% and 17–61% of the "P-replete" and "P-stress" *T. weissflogii* batches, respectively (Fig. 5; Table 4).

4. Discussion

4.1. Impact of P-stress on the initial biochemical composition of T. weissflogii

Previous investigations that assessed the impact of P-stress on diatoms observed increases in their absolute carbon (pmol C $cell^{-1}$), probably attributed to the biosynthesis of sulfolipids and betaine lipids (Obata et al., 2013; Brembu et al., 2017), and occasionally in their nitrogen (pmol N $cell^{-1}$) content (Lynn et al., 2000; Chauton et al., 2013). The results of this study agree with the general increase of C and N content and confirm that a P-stress may strongly affect the carbon and nitrogen contents per cell of *T. weissflogii* (Table 1). Our results also showed a decrease in the $bSiO_2$ content due to P-stress, which was also reflected in the Si/C and Si/N ratios (Table 1). It is generally admitted that a decrease in the growth rate due to nutrient stress other than Si-limitation leads to an increase of the cellular $bSiO_2$ content (Martin-Jézéquel et al. 2000, Claquin et al. 2002). However, low Si quotas have sometimes been measured for nutrient-stressed diatoms in *in situ* or laboratory studies, which may partially be explained by the simultaneous decrease of the *T. weissflogii* cellular volume (Bucciarelli et al. 2010; Lasbleiz et al. 2014; Suroy et al., 2015; Boutorh et al., 2016). These results are contrary to what has been measured for *T. pseudonana* (Claquin et al., 2002) but agree well with

437 what has been observed for *T. weissflogii* (De La Rocha et al., 2010), emphasizing the
438 idea that diatoms of the same genus may have a different physiological response to
439 environmental stress.

440 The elemental ratios of the "P-replete" cells were similar to those reported in the
441 literature (Redfield et al., 1963; Brzezinski, 1985; Sarthou et al., 2005), with C/N of 6.7,
442 Si/N of 1.1, and Si/C of 0.17. P-stress induced a decrease of the Si/N and Si/C ratios
443 from 1.1 to 0.46, and from 0.17 to 0.08, respectively, which is similar to what has been
444 observed for N- and Si- limitations stress (Suroy et al., 2015). In our study, P-stress
445 induced a slight decrease in the C/N ratio from 6.7 to 6 (Table 1). Contrarily, most
446 previous studies observed an increase in C/N ratios under nutrient stress especially for
447 N- and Si- stress (Suroy et al., 2015; De La Rocha et al., 2010). However, a recent study
448 by Clark et al. (2014) illustrated very well the strong variability of C/N ratios under P-
449 limitation stress for *T. weissflogii*. The variability of this ratio may be explained by an
450 irregular excretion of polysaccharides to regulate the C/N ratios of diatom cells (Suroy
451 et al. 2015).

452 The PCHO concentrations in the "P-replete *T. weissflogii*" batch were lower
453 than those found in the "P-stress *T. weissflogii*" batch, accounting for 14% and 16% of
454 POC, respectively (Table 2). The carbohydrate data presented here agree with those of
455 previous investigations that assessed the impact of P-stress in *T. pseudonana* after
456 analyzing its carbohydrate and lipid components (Harrison et al., 1990b; Urbani et al.,
457 2005). Moreover, our results are consistent with the potential regulation of glycolysis
458 that has been observed in similar diatoms (e.g., *T. pseudonana*) that face strong
459 phosphate limitation (Dyhrman et al., 2012).

460 At the molecular level, the carbon allocation towards the carbohydrate
461 component under "P-stress *T. weissflogii*" conditions was mainly reflected by the
462 largest proportions of glucose, galactose, and xylose (Table 2). Galactose and xylose are
463 generally found as parts of structural, extracellular heteropolysaccharides, whereas
464 glucose is derived from both structural and storage (β–1,3 glucan; e.g., chrysolaminarin)
465 compounds in diatoms (Haug and Myklestad, 1976; Hicks et al., 1994; Chiovitti et al.,
466 2003; Størseth et al., 2005). Although the carbohydrate analysis presented here does not
467 allow for the differentiation of the origin of glucose (i.e., storage vs. structural
468 monosaccharide), the high levels of glucose, galactose, and xylose most likely reflect
469 the excretion and rapid degradation of structural polysaccharides under P-stress
470 conditions (Magaletti et al., 2004; Ai et al., 2015). It is worth noting that high glucose
471 and xylose levels have also been reported under "N-stress" conditions for *T. weissflogii*
472 (Suroy et al., 2015). The most striking result of this study is the low relative abundance
473 of ribose in the "P-stress" experiment (4.3% of PCHO) compared to the "P-replete *T.*
474 *weissflogii*" experiment (19.5% of PCHO; Table 2), which further suggests the better
475 physiological status of *T. weissflogii* cells, and the presence of ribose–containing
476 molecules (*e.g.*, DNA and ATP) under "P-replete *T. weissflogii*" conditions. This result
477 is consistent with previous investigations that assessed N- and Si-stress in *T. weissflogii*
478 cells and showed low ribose levels (Suroy et al., 2015).
479
480 *4.2. Effect of P-stress on the degradation of* T. weissflogii *organic matter, $bSiO_2$*
481 *dissolution, and PCHO* T. weissflogii *dynamics*

482 The kinetic calculations of the POC and PON degradation of *T. weissflogii*
483 grown under P-replete or P-stress conditions, suggest the presence of two pools of

484 organic matter: one that exhibited high degradation during the first 7–8 days, and a
485 second, less degradable pool that showed no degradation ($k_2 = 0$ for model 2b) and left
486 behind a so-called “recalcitrant” component (Table 3; Fig. 3). Such a feature has already
487 been well-documented for different types of organic matter, including fresh
488 phytoplanktonic cultures (Westrich and Benner, 1984; Harvey et al., 1995; Sempéré et
489 al., 2000; Moriceau et al., 2009). In an earlier study on *T. weissflogii* degradation under
490 Si- and N-stress conditions (Suroy et al., 2015), it was observed that the second-order
491 degradation rate constant (i.e., k_2) was almost equal to zero ($k_1 >> k_2 \approx 0$), which agrees
492 with the data presented in Table 3. Moreover, and similarly to N-stressed *T. weissflogii*
493 (Suroy et al., 2015), the degradation rate constants for POC and PON were higher for
494 the *T. weissflogii* grown under “P-replete” conditions than those grown under “P-stress”
495 conditions, suggesting that nutrient growth conditions (herein the availability of P) also
496 impact the degradation of photosynthesized organic matter. Degradation rates of POC
497 and PON also indicated that N-containing organic molecules disappear more rapidly
498 when they are produced by *T. weissflogii* cells grown under the presence of P (Table 3).
499 Moreover, while the pool of degradable material was more rapidly utilized in the “P-
500 replete *T. weissflogii*” batch than in the “P-stress *T. weissflogii*” batch, the contribution
501 of the non-degradable pool to the global PON and POC was similar in both batches
502 (Fig. 3). Overall, the results showed that the diatom-organic matter resulting from a P-
503 stress environment might be less labile than the diatom-organic matter produced in
504 nutrient-replete surface layers. Therefore, if P limits diatom growth, diatom-organic
505 matter is less susceptible to degradation despite the fact that similar amount of total
506 PON and POC may reach the mesopelagic/bathypelagic layers after 21 days of
507 degradation (Fig. 3).

In contrast to with POC and PON, which degraded less rapidly under "P-stress" conditions, $bSiO_2$ showed a higher dissolution in the "P-stress" experiment (Table 3). Indeed, we measured a dissolution rate constant twice faster in the "P-stress *T. weissflogii*" batch than in the "P-replete *T. weissflogii*" batch. The FTIR spectra of the frustule cleaned from the organic coating showed that more organic matter was associated to the "P–replete" than to the "P–stress" frustule (Soler, 2010; Fig. S2). This result strongly suggests that when silica frustules are closely associated with a high amount of organic matter, $bSiO_2$ dissolution rate (as shown by FTIR spectra) is slowed down which agrees with a similar study performed in our lab on *Pseudonitzschia delicatissima* (Boutorh, 2014). Indeed, the $bSiO_2$ dissolution involves a reaction between the silanol group of the frustules and a water molecule. Therefore, a high amount of organic matter associated to the frustules may reduce the access to the reactive silanol groups, which further decreases the $bSiO_2$ dissolution rate (Loucaides et al. 2010). Overall, these results suggest that $bSiO_2$ produced under "P-stress" contains less organic matter and is less resistant to dissolution. The ballast effect of the $bSiO_2$ may, therefore be decreased initially because of the low Si/C ratios (Armstrong et al., 2002; Armstrong et al., 2009; Tréguer et al., 2018; Table 1) resulted from "P-stress" and secondly because $bSiO_2$ dissolves more rapidly in "P-stress" than in "P-replete" *T. weissflogii* batches.

The rapid degradation of PCHO observed for the "P–stress *T. weissflogii*" experiment (Table 3) implies an allocation of excess carbon toward highly energetic molecules (i.e., carbohydrates), which can easily be assimilated after enzymatic hydrolysis (Fig. 4b). At the molecular level, this finding was mainly reflected in the contents of galactose, glucose, mannose, and xylose, which were among the most

abundant compounds (Table 2). The elevated concentrations of galactose, accompanied by xylose and glucose, and mannose, in the "P-stress *T. weissflogii*" batch when compared to the "P-replete *T. weissflogii*" batch most likely indicate the biosynthesis and/or excretion of structural polysaccharides during diatom growth under "P-stress *T. weissflogii*" conditions. The above monosaccharides are known to constitute the building blocks of structural polysaccharides (i.e., heteropolysaccharides) and are rapidly degraded by prokaryotes (Table 2; Fig. 5). Alternatively, these structural polysaccharides may contribute to building up the extracellular pool of EPS (Myklestad, 1977; Urbani et al., 2005; Passow, 2002), rich in glucose (Waite et al. 1995), and are the precursors of transparent exopolymer particles (TEP). In turn, TEP may trigger the formation of large, fast-sinking aggregates that are known to increase C export (Passow, 2002; Moriceau et al., 2007; Seebah et al., 2014; Chen et al., 2015).

In contrast to the above monosaccharides, ribose exhibited higher degradation rates in the "P-replete *T. weissflogii*" degradation experiment than in the "P-stress *T. weissflogii*" degradation experiment. This result, in conjunction with the elevated concentrations of ribose in the "P-replete" experiment, points toward a high lability of *T. weissflogii* organic material (note that ribose may be considered as a good proxy of fresh organic material as it is mostly found in metabolically active organisms), and a subsequent better degradation "behavior" of prokaryotes when *T. weissflogii* cells are grown under the presence of P (Table 2). Moreover, the exhaustion of ribose during the growth of *T. weissflogii* in the absence of P resulted in little bioavailability of these energy-rich ATP-containing molecules during degradation, as suggested by their low degradation rates (Table 4). A similar observation was made for ribose under N- and Si-stress conditions during the degradation of *T. weissflogii* (Suroy et al., 2015).

5. Conclusions

This study showed that "P-stress *T. weissflogii*" conditions induced an increase in the contents of POC and PON in the *T. weissflogii* cells, with a concomitant decrease in their silicon content ($bSiO_2$). The initial *T. weissflogii* chemical composition in the "P-stress" cells was characterized by high abundances of glucose (19% of PCHO), galactose (23%), and xylose (21%) compared to the "P-replete" cells, which were dominated by ribose (20% of PCHO). These results clearly suggest that "P-stress *T. weissflogii*" conditions cause changes in carbon allocation toward the carbohydrate component (i.e., synthesis of storage/structural polysaccharides). The modeling of *T. weissflogii* degradation in terms of bulk organic matter (POC, PON, and $bSiO_2$) indicated that the degradation rate constants for POC and PON were always higher in the "P-replete *T. weissflogii*" experiment (k_1 = 0.27–0.40 d^{-1}) than in the "P-stress *T. weissflogii*" experiment (k_1 = 0.19–0.17 d^{-1}). Contrarily, $bSiO_2$ formed under "P-stress *T. weissflogii*" conditions dissolved more rapidly than $bSiO_2$ produced under "P-replete *T. weissflogii*" conditions as the latter contains more organic matter strongly associated to the frustule. Overall, our study illustrates the critical role that P plays in the degradation of diatom organic matter and its impact on silica frustule dissolution and carbohydrate decomposition. Although further investigations are needed with different types of diatoms in order to make any generalizations, it appears that P-limitation on diatom growth may have important implications to the degradation of diatom–derived organic matter and, consequently, to the associated export fluxes to the ocean interior.

Acknowledgments

We thank D. Delmas for prokaryote counting during the degradation experiment and C. Labry for seawater sampling at the Brest Somlit station. The authors also acknowledge C. Soler for laboratory and field assistance and A. Masson for POC/PON measurements. This manuscript benefited from the constructive comments of two anonymous reviewers, who are also acknowledged. This study was supported by the UTIL (LEFE/CYBER, CNRS/INSU) and MANDARINE (Région Provence Alpes Côte d'Azur) projects. M. Suroy acknowledges the Aix–Marseille University for his Ph.D. scholarship.

References

Agusti, S., Gonzalez-Gordillo, J.I., Vaqué, D., Estrada, M., Cerezo, M.I., Salazar, G., Gasol, J.M., Duarte, C.M., 2015. Ubiquitous healthy diatoms in the deep sea confirm deep carbon injection by the biological pump. Nature Commun. 6:7608. DOI: 10.1038/ncomms8608.

Ai, X.-X., Liang, J.-R., Gao, Y.-H., Lo, S.C.-L., Lee, F.W.-F., Chen, C.-P., Luo, C.-S., Du, C., 2015. MALDI-TOF MS analysis of the extracellular polysaccharides released by the diatom *Thalassiosira pseudonana* under various nutrient conditions. J. Appl. Phycol. 27, 673–684.

Armstrong, R.A., Lee, C., Hedges, J.I., Honjo, S., Wakeham S.G., 2002. A new, mechanistic model for organic carbon fluxes in the ocean based on the quantitative association of POC with ballast minerals. Deep-Sea Res II 49, 219–236.

Armstrong, R.A., Peterson, M.L., Lee, C., Wakeham, S.G., 2009. Settling velocity spectra and the ballast ratio hypothesis. Deep Sea Res. Part II 56: 1470–1478.

602 Beardall, J., Berman, T., Heraud, P., Kadiri, M. O., Light, B. R., Patterson, G., et al.
603 2001. A comparison of methods for detection of phosphate limitation in
604 microalagae. Aquat. Sci. 63, 107–121.
605 Berg, J.M., Tymoczko, J.L., Stryer, L., 2002. Biochemistry. 5th edition, New York.
606 Brembu, T., Muhlrorth, A., Alipanah, L., Bones, A. M., 2017. The effects of
607 phosphorus limitation on carbon metabolism in diatoms. Phil. Trans. R. Soc. B
608 372: 20160406.http://dx.doi.org/10.1098/rstb.2016.0406
609 Boop, L., Aumont, O., Cadule, P., et al. 2005. Response of diatoms distribution to
610 global warming and potential implications: A global model study. Geophys. Res.
611 Lett. 32. https://doi. 10.1029/2005GL023653.
612 Boutorh, J., 2014. Impact des conditions nutritionnelles sur la dissolution de la silice
613 biogénique des diatomées à travers l'étude de la variabilité de la structure
614 biphasique du frustule. Ph.D. dissertation, Université de Bretagne Occidentale,
615 France, pp 14.
616 Boutorh, J., Moriceau, B., Gallinari, M., Ragueneau, O., Bucciarelli, E., 2016. Effect of
617 trace metal-limited growth on the postmortem dissolution of the marine diatom
618 Pseudo-nitzschia delicatissima. Global Biochem. Cy. 30, 57-69. DOI:
619 10.1002/2015GB005088
620 Brzezinski, M.A., 1985. The Si:C:N ratio of marine diatoms : interspecific variability
621 and the effet of some environmental variables. J. Phycol. 21, 347–57.
622 Bucciarelli, E., Pondaven, P., Sarthou, G., 2010. "Effects of an iron-light co-limitation
623 on the elemental composition (Si, C, N) of the marine diatoms *Thalassiosira*
624 *oceanica* and *Ditylum brightwellii*." Biogeosciences 7, 657–669.

625 Chauton, M.S., Olsen, Y., Vadstein, O., 2013. Biomass production from the microalga
626 *Phaeodactylum tricornutum*: Nutrient stress and chemical composition in
627 exponential fed-batch cultures. Biomass and bioenergy 58, 87–94.
628 Chen, J., Thornton, D.C.O., 2015. Transparent exopolymer particle production and
629 aggregation by a marine planktonic diatom (*Thalassiosira weissflogii*) at different
630 growth rates. J. Phycol. 51, 381-393.
631 Chiovitti, A., Higgins, M.J., Harper, R.E., Wetherbee, R., 2003. The complex
632 polysaccharides of the raphid diatom Pinnularia viridis (*Bacillariophyceae*). J.
633 Phycol. 39, 543–554.
634 Claquin, P., Martin-Jézéquel, V., Kromkamp, J.C., Veldhuis, M. J. W., Kraay, G. W.,
635 2002. Uncoupling of silicon compared to carbon and nitrogen metabolism, and role
636 of the cell cycle, in continuous cultures of *Thalassiosira pseudonana*
637 (bacillariophyceae) under light, nitrogen and phosphorus control. J. Phycol. 38,
638 922–930.
639 Clark, D. R., Flynn, K. J., Fabian, H., 2014. Variation in elemental stoichiometry of the
640 marine diatom *Thalassiosira weissflogii* (Bacillariophyceae) in response to
641 combined nutrient stress and changes in carbonate chemistry. J. Phycol. 50, 640–
642 651. doi:10.1111/jpy.12208.
643 De La Rocha, C.L., Terbrüggen, A., Völker, C., Hohn, S., 2010. Response to and
644 recovery from nitrogen and silicon starvation in *Thalassiosira weissflogii*: growth
645 rates, nutrient uptake and C, Si and N content per cell. Mar. Ecol. Prog. Ser. 412,
646 57–68.

Diekmann, A.B.S., Peck, M.A., Holste, L., St John, M.A., Campbell, R.W., 2009. Variation in diatom biochemical composition during a simulated bloom and its effect on copepod production. J. Plankton Res. 31, 1391–1405.

Downing, J.A., 1997. Marine nitrogen: Phosphorus stoichiometry and the global N:P cycle. Biogeochemistry 37, 237–252.

Duhamel, S., Moutin, T., Van Wambeke, F., Van Mooy, B., Raimbault, P., Chaustre, H., 2007. Growth and specific P-uptake rates of bacterial and phytoplanktonic communities in the Southeast Pacific (BIOSOPE cruise). Biogeosciences 4, 941–956.

Dyhrman, S.T., Jenkins, B.D., Rynearson, T.A., Saito, M.A., Mercier, M.L., Alexander, H., Whitney, L.P., Drzewianowski, A., Bulygin, V.V., Bertrand, E.M., Wu, Z., Benitez-Nelson, C., Heithoff, A., 2012. The transcriptome and proteome of the diatom *Thalassiosira pseudonana* reveal a diverse phosphorus stress response. PloS one, 7, e33768. htpps://doi.org/10.1371/journal.pone.0033768.

Engel, A., Abramson, L., Szlosek, J., Liu, Z., Stewart, G., Hirschberg, D., Lee, C., 2009. Investigating the effect of ballasting by $CaCO_3$ in *Emiliania huxleyi*, II: Decomposition of particulate organic matter. Deep-Sea Res. II 56, 1408–1419. DOI:10.1016/j.dsr2.2008.11.028

Gärdes, A., Iversen, M. H., Grossart, H. P., Passow, U., Ullrich, M. S., 2010. Diatom-associated bacteria are required for aggregation of *Thalassiosira weissflogii*. ISME J. 5, 436–445.

668 Godwin, C.M., Cotner, J.B., 2015 Aquatic heterotrophic bacteria have highly flexible
669 phosphorus content and biomass stoichiometry. ISME J.
670 https://doi:10.1038/ismej.2015.34
671 Gordon, L.I., Jennings, J.C., Ross, A.A., Krest, J.M., 1993. A suggested protocol for
672 continuous flow automated analysis of seawater nutrients. In Group, C. o. [Ed.]
673 OSU, College of Oc. Descriptive. Chem. Oc. Grp. Tech. Rpt. OSU College of
674 Oceanography Descriptive, Corvallis, pp. 1–55.
675 Goutx, M., Wakeham, S.G., Lee, C., Duflos, M., Guigue, C., Liu, Z., Moriceau, B.,
676 Sempéré, R., Tedetti, M., Xue, J., 2007. Composition and degradation of marine
677 particles with different settling velocities in the northwestern Mediterranean Sea.
678 Limnol. Oceanogr. 52, 1645–64.
679 Grattepanche, J-D., Vincent, D., Breton, E., Christaki, U., 2011. Microzooplankton
680 herbivory during the diatom–Phaeocystis spring succession in the eastern English
681 Channel. J. Exp. Mar. Biol. Ecol. 404, 87–97.
682 Greenwood, J.E., Truesdale, V.W., Rendell, A.R., 2001. Biogenic silica dissolution in
683 seawater - in vitro chemical kinetics. Prog. Oceanogr. 48, 1–23.
684 Gruber, N., Galloway, J.N., 2008. An Eath-system perspective of the global nitrogen
685 cycle. Nature, 451, 293-96. https://doi:10.1038/nature06592.
686 Guillard, R.R.L., Ryther, J.H., 1962. Studies of marine planktonic diatoms. I. Cyclotella
687 nana hustedt and Detonela confervacea (cleve) gran. Can. J. Microbiol. 8, 229–
688 239.
689 Guillard, R.R.L., 2005. Purification methods for microalgae, in: Andersen, R.A (Ed.)
690 Algal Culturing Techniques. Elsevier Academic Press, Burlington, MA, USA, pp.
691 117–132.

692 Harrison, P.J., Hu, M.H., Yang, Y.P., Lu, X., 1990a. Phosphate limitation in estuarine
693 and coastal waters of China. J. Exp. Mar. Biol. Ecol. 140, 79-87. DOI:
694 10.1016/0022-0981(90)90083-O.
695 Harrison, P.J., Thompson, P.A., Calderwood, G.S., 1990b. Effects of nutrient and light
696 limitation on the biochemical composition of phytoplankton. J. Appl. Phycol. 2,
697 45–56.
698 Harvey, H.R., Tuttle, J.H., Bell, J.T., 1995. Kinetics of phytoplankton decay during
699 simulated sedimentation: Changes in biochemical composition and microbial
700 activity under oxic and anoxic conditions. Geochim. Cosmochim. Acta 59, 3367–
701 77.
702 Harvey, H.R., Macko, S.A., 1997. Kinetics of phytoplanktondecay during simulated
703 sedimentation: changes in lipids under oxic and anoxic conditions. Org. Geochem.
704 129–140.
705 Haug, A., Myklestad, S.M., 1976. Polysaccharides of marine diatoms with special
706 reference to Chaetoceros species. Mar. Biol. 34, 217–22.
707 Hicks, R.A., Owen, C.J., Aas, P., 1994. Deposition, resuspension, and decomposition of
708 particulate organic matter in sediments of lake Itasca, Minnesota, USA.
709 Hydrobiologia 284,79–91.
710 Jackson, G.A., Williams, P.M., 1985. Importance of dissolved organic nitrogen and
711 phosphorus to biological nutrient cycling. Deep-Sea Res 32, 223–35.
712 Kamatani, A., Riley, J.P., 1979. Rate of dissolution of diatom silica walls in seawater.
713 Mar. Biol. 55, 29–35.
714 Kamatani, A., Riley, J.P., Skirrow, G., 1980. The dissolution of opaline silica of of
715 diatom tests in seawater. J. Oceanogr. Soc. Jpn 36, 201–8.

716 Kamatani, A., 1982. Dissolution rates of silica from diatoms decomposing at various
717 temperature. Mar. Biol. 68, 91–96.
718 Karl, D.M., Björkman, K,M., 2015. Dynamics of dissolved organic phosphorus, in:
719 Hansell, D.A., Carlson, C.A., (Eds.) Biogeochemistry of marine dissolved organic
720 matter. Academic Press, New York. pp. 233–318.
721 Lasbleiz, M., Leblanc, K., Blain, S., Ras, J., Cornet-Barthaux, V., Hélias Nunige,
722 S., Quéguiner, B., 2014. Pigments, elemental composition (C, N, P, Si) and
723 stoichiometry of particulate matter, in the naturally iron fertilized region of
724 Kerguelen in the Southern Ocean, Biogeosciences 11, 5931–5955,
725 doi.org/10.5194/bg-11-5931-2014.
726 Lehninger, A.L., Nelson, D.L., Cox, M.M., 1993. Principles of Biochemistry, 2nd ed.
727 Worth Publishers, New York.
728 Liu, S., Guo, Z.L., Li, T., Huang, H., Lin, S.J., 2011. Photosynthetic efficiency, cell
729 volume, and elemental stoichiometric ratios in *Thalassirosira weissflogii* under
730 phosphorus limitation. Chinese J. Oceanol. Limnol. 29, 1048–56.
731 Loucaides, S., Behrends, T., Van Cappellen, P., 2010. Reactivity of biogenic silica:
732 surface *vs* bulk charge density. Geochim. Cosmochim. Acta 74, 517–530.
733 Lynn, S.G., Kilham, S.S., Kreeger, D.A., Interlandi, S.J., 2000. Effect of nutrient
734 availability on the biochemical and elemental stoichiometry in the freshwater
735 diatom Stephanodiscus minutulus (*Bacillariophyceae*). J. Phycol. 36, 510–22.
736 Magaletti, E., Urbani, R., Sist, P., Ferrari, C.R., Cicero, A.M., 2004. Abundance and
737 chemical characterization of extracellular carbohydrates released by the marine
738 diatom *Cylindrotheca fusiformis* under N- and P- limitation. Eur. J. Phycol. 39,
739 133–42.

740 Marie, D., Partensky, F., Jacquet, S., Vaulot, D., 1997. Enumeration and cell cycle
741 analysis of natural populations of marine picoplankton by flow cytometry using the
742 nucleic acid stain SYBR Green I. Appl. Environ. Microbiol. 63, 186–93.
743 Marie, D., Partensky, F., 2006. Analyse des micro-organismes marin. In La cytométrie
744 en flux, Lavoisier, Edition Tec and Doc; Ronot, R., Grunwald, D., Mayol , J.-F.,
745 Boutonnat, J., coordonateurs, p. 210–33.
746 Moore, C.M., Mills, M., Langlois, R., Milne, A., Achterberg, E.P., La Roche, J., Geider,
747 R.J., 2008. Relative influence of nitrogen and phosphorus availability on
748 phytoplankton physiology and productivity in the oligotrophic sub-tropical North
749 Atlantic Ocean. Limnol. Oceanogr. 53, 291–305.
750 Moore, C.M., Mills, M.M., Arrigo, K.R., Berman-Frank, I., Bopp, L., Boyd, P.W.,
751 Galbraith, E.D., Geider, R.J., Guieu, C., Jaccard, S.L., Jickells, T.D., La Roche, J.,
752 Lenton, T.M., Mahowald, N.M., Maranon, E., Marinov, I., Moore, J.K.,
753 Nakatsuka, T., Oschlies, A., Saito, M.A., Thingstad, T.F., Tsuda, A., Ulloa O.,
754 2013. Processes and patterns of oceanic nutrient limitation. Nat. Geosci. 6: 701-
755 710. doi: 10.1038/NGEO1765.
756 Moriceau, B., Gallinari, M., Soetaert, K., Ragueneau, O., 2007. Importance of particle
757 formation to reconstructed water column biogenic silica fluxes. Glob. Biogeochem.
758 Cycles 21, GB3012. doi:10.1029/2006GB002814.
759 Moriceau, B., Goutx, M., Guigue, C., Lee, C., Armstrong, R.A., Duflos, M., Tamburini,
760 C., Charrière, B., Ragueneau, O., 2009. Si–C interactions during degradation of the
761 diatom *Skeletonema marinoi*. Deep-Sea Res. II 56,1381–95.
762 Myklestad, S.M., 1977. Production of carbohydrates by marine planktonic diatoms. 2.
763 Influence of N/P ratio in growth medium on assimilation ratio, growth rate, and

764 production of cellular and extracellular carbohydrates by *Chaetocearos affinis* var
765 Willei (Gran) Hustedt and Skele. J. Exp. Mar. Biol. Ecol. 29:161–79.
766 Némery, J., Garnier, J., 2016. The fate of phosphorus. Nature Geosci. 9, 343–344.
767 Nieuwenhuize, J., Maas, Y.E.M., Middelburg, J.J., 1994. Rapid analysis of organic
768 carbon and nitrogen in particulate materials. Mar. Chem. 45, 217–24.
769 Obata, T., Fernie, A.I., Nunes-Nesi, A., 2013. The Central Carbon and Energy
770 Metabolism of Marine Diatoms. Metabolites, 3, 325–346;
771 doi:10.3390/metabo3020325.
772 Palmucci, M., Ratti, S., Giordano, M., 2011. Ecological and evolutionary implications
773 of carbon allocation in marine phytoplankton as a function of nitrogen availability:
774 a fourier transform infrared spectroscopy approach. J. Phycol. 47, 313–323.
775 Panagiotopoulos, C., Sempéré, R., Obernosterer, I., Striby, L., Goutx, M., Van
776 Wambeke, F., Gautier, S., Lafont, R., 2002. Bacterial degradation of large particles
777 in the southern Indian Ocean using in vitro incubation experiments. Org. Geochem.
778 33, 985–1000.
779 Panagiotopoulos, C., Sempéré, R., 2007. Sugar dynamics in large particles during in
780 vitro incubation experiments. Mar. Ecol. Prog. Ser. 330, 67–74.
781 Panagiotopoulos, C., Sempéré, R., Para, J., Raimbault, P., Rabouille, C., Charrière, B.,
782 2012. The composition and flux of particulate and dissolved carbohydrates from
783 the Rhone River into the Mediterranean Sea. Biogeosciences 9, 1827–1844.
784 Panagiotopoulos, C., Wurl, O., 2009. Spectrophotometric and chromatographic analysis
785 of carbohydrates in marine samples, in: Wurl, O., (Ed.) Practical Guidelines for the
786 Analysis of Seawater. Taylor and Francis, Boca Raton, FL, pp. 49–65.

787 Passow, U., 2002. Production of transparent exopolymer particles (TEP) by phyto- and
788 bacterioplankton, Mar. Ecol. Prog. Ser. 236, 1–12.
789 Piontek, J., Handel, N., Langer, G., Wohlers, J., Riebesell, U., Engel, A., 2009. Effects
790 of rising temperature on the formation and microbial degradation of marine diatom
791 aggregates. Aquat. Microb. Ecol. 54, 305-318. DOI: 10.3354/ame01273.
792 Paytan, A., McLaughlin, K., 2007. The oceanic phosphorus cycle. Chem. Rev. 107,
793 563–76.
794 Ragueneau, O., Treguer, P., 1994. Determination of biogenic silica in coastal
795 waters:Applicability and limits of alkaline digestion method. Mar. Chem. 45, 43–
796 51.
797 Redfield, A.C., Ketchum, B.H., Richards, F.A., 1963. The influence of organisms on the
798 composition of sea water, in: Hill, M.N., (Ed.) The sea: ideas and observations on
799 progress in the study of the seas. Interscience, New York, pp 26–77.
800 Ryther, J.H., Dunstan, W.H., 1971. Nitrogen, phosphorus and eutrophication in the
801 coastal marine environment. Science 171:1008–13.
802 Sarthou, G., Timmermans, K.R., Blain, S., Tréguer, P., 2005. Growth physiology and
803 fate of diatoms in the ocean: a review. J. Sea Res. 53, 25–42. DOI:
804 10.1016/j.seares.2004.01.007.
805 Schreiber, U., Schliwa, U., Bilger, W., 1986. Continuous recording of photochemica
806 and nonphotochemical chlorophyll fluorescence quenching with a new type of
807 modulation fluorometer. Photosynth. Res. 10, 51–62.
808 Sebastian, M., Smith, A.F., Gonzalez, J.M., Fredricks, H.F., et al. 2016. Lipid
809 remodeling is a widespread strategy in marine heterotrophic bacteria upon

phosphorus deficiency. ISME journal. 10, 968-78. https://doi: 10.1038/ismej.2015.172

Seebah, S., Fairfield, C., Ullrich, M.S., Passow, U., 2014. Aggregation and Sedimentation of *Thalassiosira weissflogii* (diatom) in a Warmer and More Acidified Future Ocean. Plos One 9. https:// doi: 10.1371/journal.pone.0112379.

Sempéré, R., Yoro, S-C., Van Wambeke, F., Charrière, B., 2000. Microbial decomposition of large organic particles in the northwestern Mediterranean Sea: an experimental approach. Mar. Ecol. Prog. Ser. 198, 61–72.

Shifrin, N.S., Chisholm, S.W., 1981. Phytoplankton lipids interspecific differences and effects of nitrate, silicate and light-dark cycles. J. Phycol. 17, 374-84.

Smetacek, V., 1985. Role of sinking in diatom life-history cycles: ecological, evolutionary and geological significance. Mar. Biol. 84, 239–251.

Soler, C., 2010. Impact des conditions de croissance sur le métabolisme et les interactions Si-OC des diatomées– conséquences sur la vitesse de reminéralisation de la silice biogène et de la matière organique. Ph.D. dissertation, Université de Bretagne Occidentale, France, pp. 207.

Størseth, T.R., Hansen, K., Reitan, K.I., Skjermo, J., 2005. Structural characterization of β-D-(1→3)-glucans from different growth phases of the marine diatoms *Chaetoceros mülleri* and *Thalassiosira weissflogii*. Carbohyd. Res. 340:1159–64.

Sun, M.Y., Lee, C., Aller, R.C., 1993. Anoxic and oxic degradation of C-14-labeled chloropigments and a C-14-labeled diatom in long-island sound sediments. Limnol. Ocenogr. 38, 1438–1451.

832 Suroy, M., Panagiotopoulos, C., Boutorh, J., Goutx, M., Moriceau, B., 2015.
833 Degradation of diatom carbohydrates: A case study with N– and Si– stressed
834 *Thalassiosira weissflogii*. J. Exp. Mar. Biol. Ecol. 470, 1–11.
835 Tanaka, T., Thingstad, T.F., Christaki, U., Colombet, J., et al. 2011. Lack of P-
836 limitation of phytoplankton and heterotrophic prokaryotes in surface waters of
837 three anticyclonic eddies in the stratified Mediterranean Sea. Biogeosciences 8,
838 525-38. DOI: 10.5194/bg-8-525-2011.
839 Thingstad, T.F., Krom, M.D., Mantoura, R.F.C., Flaten, G.A.F, Groom, S., et al. 2005.
840 Nature of phosphorus limitation in the ultraoligotrophic eastern Mediterranean.
841 Science 309:1068–71.
842 Tréguer, P., Bowler, C., Moriceau, B., Dutkiewicz, et al. 2018. Influence of diatom
843 diversity on the ocean biological carbon pump. Nature Geoscience 1: 27–37. DOI:
844 10.1038/s41561-017-0028-x.
845 Trommer, G., Leynaert, A., Klein, C., Naegelen, A., Beker, B., 2013. Phytoplankton
846 phosphorus limitation in a North Atlantic coastal ecosystem not predicted by
847 nutrient load. J. Plankton Res. 35:1207-1219. doi:10.1093/plankt/fbt070.
848 Troussellier, M., Courties, C., Vaquer, A., 1993. Recent applications of flow cytometry
849 in aquatic microbial ecology. Biol. Cell 78, 111–21.
850 Urbani, R., Magaletti, E., Sist, P., Cicero, A.M., 2005. Extracellular carbohydrates
851 released by the marine diatoms *Cylindrotheca closterium*, *Thalassiosira*
852 *pseudonana* and *Skeletonema costatum*: effect of P-depletion and growth status.
853 Sci. Total Env. 353, 300–6.

Van Mooy, B.A.S., Fredricks, H.F., Pedler, B.E., Dyhrman, S.T., et al (2009) Phytoplankton in the ocean use non-phosphorus lipids in response to phosphorus scarcity. Nature 458: 69–72.

Vitousek, P.M., Howarth, R.W., 1991. Nitrogen limitation on land and in the sea: How can it occur? Biogeochemistry 13, 87–115.

Waite, A.M., Bienfang, P., Harrison, P.J., 1992. Spring bloom sedimentation in a sub-arctic ecosystem.1. Nutrient sensitivity. Mar. Biol. 114, 119–29.

Westrich, J., Berner, R., 1984. The role of sedimentary organic matter in bacterial sulphate reduction: the G model tested. Limnol. Oceanogr. 29, 236–49.

Wetz, M.S., Hales, B., Wheeler, P.A., 2008. Degradation of phytoplankton-derived organic matter: implications for carbon and nitrogen biogeochemistry in coastal ecosystems. Estuar. Coast. Shelf Sci. 77: 422-432. DOI: 10.1016/j.ecss.2007.10.002.

Wu, J., Sunda, W., Boyle, E.A., Karl, D.M., 2000. Phosphate depletion in the western North Atlantic Ocean. Science 289, 759–62.

ZoBell, C.E., 1941. Studies on marine bacteria. I. The cultural requirement of heterotrophic aerobes. J. Mar. Res. 4, 42–75.

Zohary, T., Herut, B., Krom, M.D., Mantoura, R.F., et al 2005. P–limited bacteria but N and P co-limited phytoplankton in the Eastern Mediterranean – a microcosm experiment. Deep Sea Res. II 52, 3011–2.

Table Captions:

Table 1. Initial parameters measured in each batch at the beginning (T_0) of the experiment. The previous assumption also considers that there is little variability in the POC, PON, and $bSiO_2$ concentrations between day 0 and day 1 of the experiment. Thus, the ratio of these parameters to the diatom cell does not change drastically between day 0 and day 1.

Table 2. Elemental carbohydrate compositions (as percentages of total sugar, mol%) and the total PCHO–C concentrations (µM) during the 21 days of degradation. The PCHO yields are given as a percentage of the total PCHO–C relative to the POC. Abbreviations: Fuc. – Fucose; Rha. – Rhamnose; Ara. – Arabinose; GlcN. – Glucosamine; Gal. – Galactose; Glc. – Glucose; Man. – Mannose; Xyl. – Xylose; Rib. – Ribose; GalUA. – Galacturonic Acid. The number of replicates is given in the caption of Fig. 4.

Table 3. Estimated kinetic parameters for POC, PON, $bSiO_2$ and PCHO during the degradation of *T. weissflogii*. The standard error (SE) is given for each estimate. Extremely significant estimates are underlined ($p < 0.0001$). Kinetic parameters (k_1, C_2) were calculated according to models 1 and 2 using equations (1) and (2b) (see statistical analysis and estimation of kinetic parameters section). k_1 and C_2 units are given in d^{-1} and µmol/µmol, respectively.

Table 4. Estimated kinetic parameters for individual monosaccharides during the biotic degradation of *T. weissflogii*. The standard error (SE) is given for each estimate.

902 Extremely significant estimates are underlined ($p < 0.0001$). Abbreviations are the same
903 as in Tables 2 and 3. Kinetic parameters (k_1 in d^{-1} and C_2 in µmol/µmol) were
904 calculated according to model 1 and/or 2 using equations (1) and/or (2b).
905
906 *Figure Captions:*
907
908 **Figure 1.** Schematic presentation of the experimental design of sampling, growth and
909 prokaryotic degradation of *T. weissflogii* cells (Fig. adapted from Suroy et al 2015).
910
911 **Figure 2**. Evolution of prokaryotic concentrations over time in the "P-replete *T.*
912 *weissflogii*" and "P-stress *T. weissflogii*" batches during the biodegradation
913 experiments. The prokaryotic concentrations correspond only to the free prokaryotes
914 that were measured in the batches. At each sampling point $n = 2$.
915
916 **Figure 3.** Time course responses of the (A) POC and (B) PON relative concentrations
917 of *T. weissflogii* in the "P-replete *T. weissflogii*" and "P-stress *T. weissflogii*" batches.
918 The relative concentrations were calculated by dividing the concentration on day t by
919 the concentration on days 0 and 2 for "P-stress *T. weissflogii*" and "P-replete *T.*
920 *weissflogii*" batches, respectively, for both POC and PON. The kinetics were estimated
921 using equation (2b) (section 2.6). Replicate subsamples ($n = 3$) for "P-replete" and "P-
922 stress" batches were performed on days 2, 6, 9, 12, and 19, and were used to feed the
923 degradation model (section 2.5). In the "P-stress" batch, only an $n = 2$ was obtained at
924 day 12 for both POC and PON.
925

926 **Figure 4.** Time course responses of the relative concentrations of (A) $bSiO_2$ and (B)
927 PCHO in the "P-replete *T. weissflogii*" and "P-stress *T. weissflogii*" batches. The
928 relative concentrations were calculated by dividing the concentration on day t by the
929 concentration on days 0 and 2 for the "P-stress *T. weissflogii*" and "P-replete *T.*
930 *weissflogii*" batches, respectively, for both $bSiO_2$ and PCHO. The kinetics were
931 estimated using equations (1) and (2b). For $bSiO_2$ degradation, replicate subsamples (n
932 = 3) were performed on days 2, 6, 9, and 19; and 2, 6, 9, 12, and 19 for the "P-replete *T.*
933 *weissflogii*" and "P-stress *T. weissflogii*" experiments, respectively. On day 12, only an
934 n = 2 was obtained for the "P-replete *T. weissflogii*" experiment. For PCHO
935 degradation, replicate subsamples (n = 3) were performed on days 6, 12, and 19 and 2,
936 6, and 19 for the "P-replete *T. weissflogii*" and "P-stress *T. weissflogii*" experiments,
937 respectively. On days 9 and 12, only an n = 2 was obtained for the "P-stress *T.*
938 *weissflogii*" experiment.
939
940 **Figure 5.** Time course responses of (A) galactose, (B) glucose, (C) xylose and (D)
941 ribose in the "P-replete *T. weissflogii*" and "P-stress *T. weissflogii*" batches. The relative
942 concentrations were calculated by dividing the concentration on day t by the
943 concentrations on day 0 and 2 for the "P-stress" and "P-replete" batches, respectively,
944 for individual monosaccharides. The kinetics were estimated using equations (1) and
945 (2b). The degradation rates, including experimental points, are given in Table 5.

Table 1.

Growth conditions	Batch volume (L)	[*T. weissflogii* cells] (cell L^{-1})	[POC] /[*T. weissflogii* cell] (pmol $cell^{-1}$)	[PON] /[*T. weissflogii* cell] (pmol $cell^{-1}$)	[Prokaryotic inoculum] (cell L^{-1})	[$bSiO_2$]/[diatom cell] (pmol $cell^{-1}$)
P-replete *T. weissflogii*	12	6.60×10^7	12.0	1.8	7.02×10^{10}	2.0
P-stress *T. weissflogii*	12	6.80×10^7	15.5	2.6	5.64×10^{10}	1.2

Table 2.

Experiment	Time (d)	Fuc.	Rha.	Ara.	GlcN.	Gal.	Glc.	Man.	Xyl.	Rib.	GalUA	PCHO–C	PCHO–C/POC
«P-replete *T. weissflogii*»	0	10.1	6.29	1.03	2.66	18.4	12.4	13.4	14.2	19.5	2.07	110	13.9
	1	8.72	5.73	0.72	4.87	16.7	16.6	15.1	12.1	16.8	2.69	112	7.23
	2	10.0	6.61	1.14	4.16	18.5	14.5	11.6	13.1	18.6	1.80	104	6.12
	4	9.29	5.11	2.06	5.14	18.6	19.5	13.6	13.4	12.5	0.93	113	8.19
	5	9.34	6.44	2.95	9.11	17.2	15.4	10.7	15.7	12.0	1.33	107	8.11
	6	11.3	7.86	2.69	5.39	16.3	18.2	10.4	14.9	12.0	0.94	83.9	7.06
	7	11.7	9.49	2.09	5.95	13.5	17.4	10.4	16.1	12.7	0.67	80.0	7.01
	10	10.8	10.5	2.28	8.32	13.1	17.5	14.0	13.9	8.85	0.82	61.3	5.78
	11	9.77	7.41	1.78	8.38	14.3	18.5	16.8	14.7	7.75	0.58	83.6	7.82
	12	7.75	9.30	1.74	8.47	14.9	18.5	18.5	13.7	6.53	0.56	89.3	9.04
	14	9.12	9.00	2.18	7.72	15.0	20.0	12.0	15.3	9.35	0.45	68.4	5.74
	16	8.92	10.1	2.86	6.37	12.1	21.5	10.1	15.4	11.4	1.31	46.1	4.32
	17	9.41	10.0	2.37	6.96	13.9	20.0	11.1	15.0	9.61	1.66	62.4	5.99
	18	8.00	8.71	3.15	5.18	14.5	21.0	13.8	16.0	8.40	1.20	80.1	7.29
	19	10.0	9.99	4.03	5.71	12.2	19.4	9.47	16.8	11.2	1.25	54.2	4.97
	20	7.64	8.42	13.2	6.39	12.2	19.0	9.74	13.3	8.73	1.35	70.6	6.47
	21	8.17	8.92	6.95	6.68	12.3	19.3	11.6	16.1	8.56	1.42	65.8	6.01
«P-stress *T. weissflogii*»	0	6.11	2.90	6.56	1.40	23.0	18.6	15.4	21.4	4.32	0.34	169	16.0
	1	8.05	4.87	3.58	1.57	20.4	24.8	16.7	13.0	6.37	0.69	97.2	9.57
	2	12.3	6.76	4.61	2.05	21.2	13.8	15.5	15.0	8.36	0.58	68.5	7.32
	5	11.7	6.06	7.11	3.44	17.3	14.8	14.0	14.1	11.1	0.39	59.3	7.42
	6	13.2	6.24	9.80	1.78	15.0	16.4	7.82	14.8	14.3	0.62	46.2	5.67
	7	11.2	6.40	5.79	3.15	18.1	20.4	9.66	14.8	10.2	0.35	73.4	9.43
	8	12.5	6.31	8.81	2.29	15.4	21.1	9.05	14.0	10.1	0.48	44.3	5.96

9	16.0	6.58	10.8	1.39	11.1	17.3	6.97	15.8	13.5	0.61	34.9	5.76
10	13.0	8.09	6.74	3.08	21.1	12.5	9.62	16.2	9.29	0.41	72.9	12.1
11	16.5	8.43	9.22	1.52	14.3	12.8	8.09	17.7	10.2	1.34	40.5	6.74
12	14.8	7.99	8.61	1.91	14.9	15.5	9.74	16.2	8.84	1.55	49.4	9.16
14	13.3	8.06	9.97	1.30	11.6	18.3	7.64	15.7	10.6	3.53	44.1	6.36
15	18.2	7.34	8.22	1.78	13.3	14.4	10.2	15.5	7.93	3.15	53.7	9.00
16	21.3	7.43	9.33	0.68	12.4	13.8	7.33	15.4	10.7	1.50	42.1	7.23
17	18.0	6.50	7.84	1.13	14.0	14.3	11.3	18.4	7.34	1.22	56.3	7.45
18	15.0	7.36	9.50	2.77	16.2	15.6	12.5	15.8	4.07	1.17	68.2	7.99
19	17.4	5.93	13.1	1.92	14.2	17.8	7.61	14.7	5.60	1.72	43.2	7.07
20	11.1	5.41	5.83	6.43	22.1	14.2	11.2	15.6	7.02	1.21	73.2	11.6
21	14.6	4.69	10.3	3.49	15.7	16.4	8.45	15.7	8.81	1.86	32.7	5.00

Table 3.

	«P-replete *T. weissflogii* »						«P-stress *T. weissflogii* »					
	k_1		C_2				k_1		C_2			
Kinetic parameters	Value	SE	Value	SE	R^2		Value	SE	Value	SE	R^2	
POC	0.40	0.05	0.62	0.01	0.94	$n = 27$	0.19	0.05*	0.54	0.03	0.87	$n = 25$
PON	0.27	0.02	0.34	0.01	0.98	$n = 27$	0.17	0.03	0.29	0.04	0.91	$n = 24$
$bSiO_2$	0.02	0.01	-	-	0.94	$n = 29$	0.05	0.02	-	-	0.95	$n = 32$
PCHO	0.15	0.08	0.55	0.08	0.66	$n = 22$	0.92	0.18	0.29	0.02	0.81	$n = 27$

* $p < 0.001$ (very significant at the 99.9% level).

Table 4

Kinetic parameteres	« P-replete *T. weissflogii* »						« P-stress *T. weissflogii* »					
	k_1		C_2				k_1		C_2			
PCHO	Value	SE	Value	SE	R^2		Value	SE	Value	SE	R^2	
Fuc.	0.08	0.03*	0.31	0.13*	0.93	$n = 21$	0	0	-	-	0	$n = 27$
Rha.	0.01	0.01	-	-	0.08	$n = 22$	0.26	0.16	0.61	0.06	0.45	$n = 24$
Ara.	0	0	-	-	0	$n = 22$	0	0	-	-	0	$n = 27$
GlcN.	0.02	0.01	-	-	0.15	$n = 22$	0.21	0.22	0.38	0.11*	0.20	$n = 26$
Gal.	0.17	0.06*	0.37	0.08*	0.77	$n = 22$	0.80	0.16	0.20	0.02	0.80	$n = 27$
Glc.	0.10	0.13	0.83	0.32	0.36	$n = 22$	0.90	0.18	0.25	0.02	0.79	$n = 27$
Man.	0.03	0.01*	-	-	0.25	$n = 22$	0.62	0.10	0.17	0.02	0.87	$n = 27$
Xyl.	0.10	0.08	0.56	0.14*	0.64	$n = 22$	1.52	0.29	0.22	0.01	0.88	$n = 27$
Rib.	0.32	0.02	0.27	0.01	0.98	$n = 22$	0.05	0.01	-	-	0.73	$n = 26$
GalUA	0.49	0.19*	0.29	0.03	0.66	$n = 22$	0	0	-	-	0.00	$n = 27$

* $p < 0.05$ (significant at the 95% level)

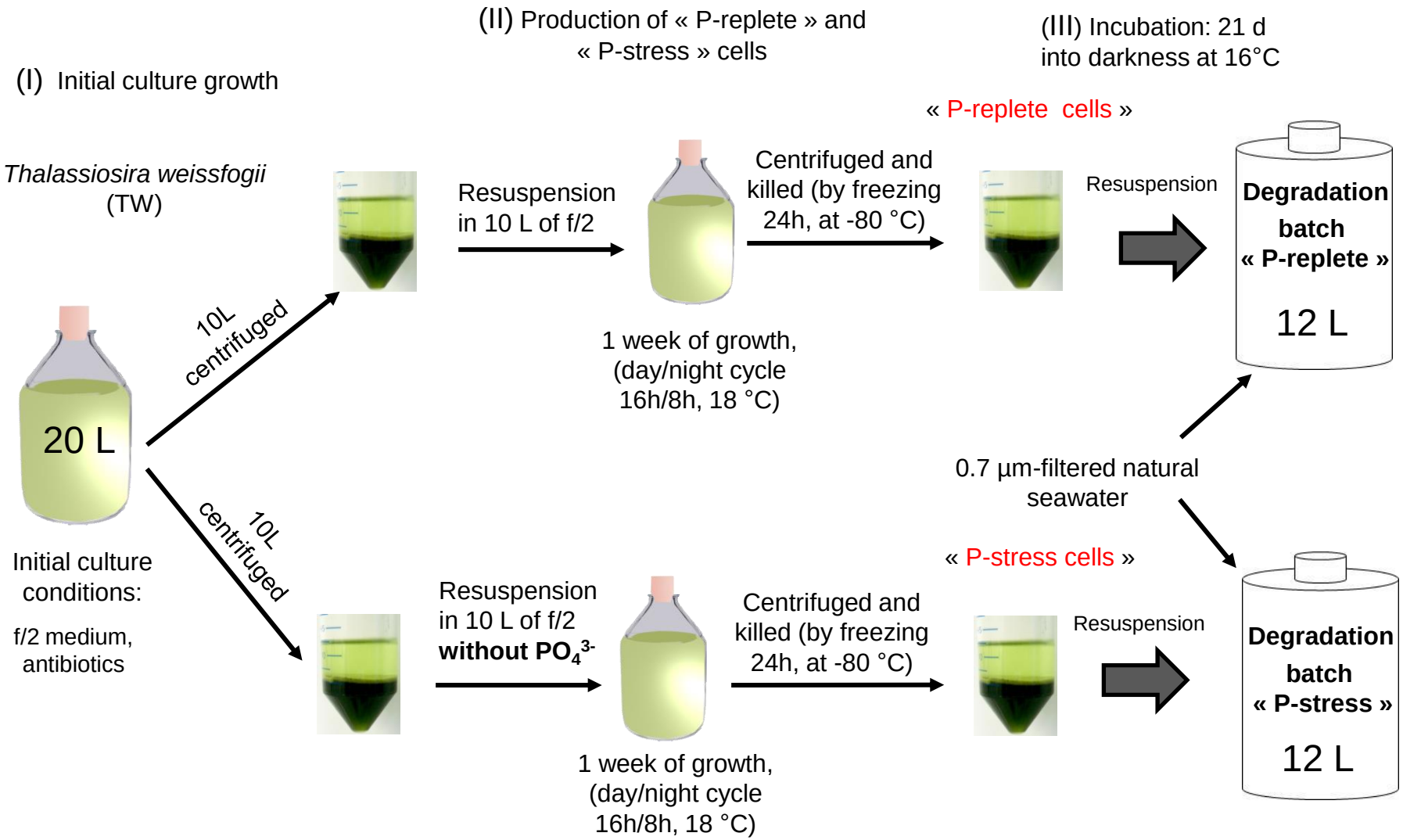
(I) Initial culture growth
(II) Production of « P-replete » and « P-stress » cells
(III) Incubation: 21 d into darkness at 16°C
Thalassiosira weissfogii (TW)
20 L
Initial culture conditions:
f/2 medium, antibiotics
10L centrifuged
10L centrifuged
Resuspension in 10 L of f/2
Resuspension in 10 L of f/2 without PO_4^{3-}
1 week of growth, (day/night cycle 16h/8h, 18 °C)
1 week of growth, (day/night cycle 16h/8h, 18 °C)
Centrifuged and killed (by freezing 24h, at -80 °C)
Centrifuged and killed (by freezing 24h, at -80 °C)
« P-replete cells »
« P-stress cells »
Resuspension
Resuspension
0.7 µm-filtered natural seawater
Degradation batch « P-replete »
12 L
Degradation batch « P-stress »
12 L

Figure 1

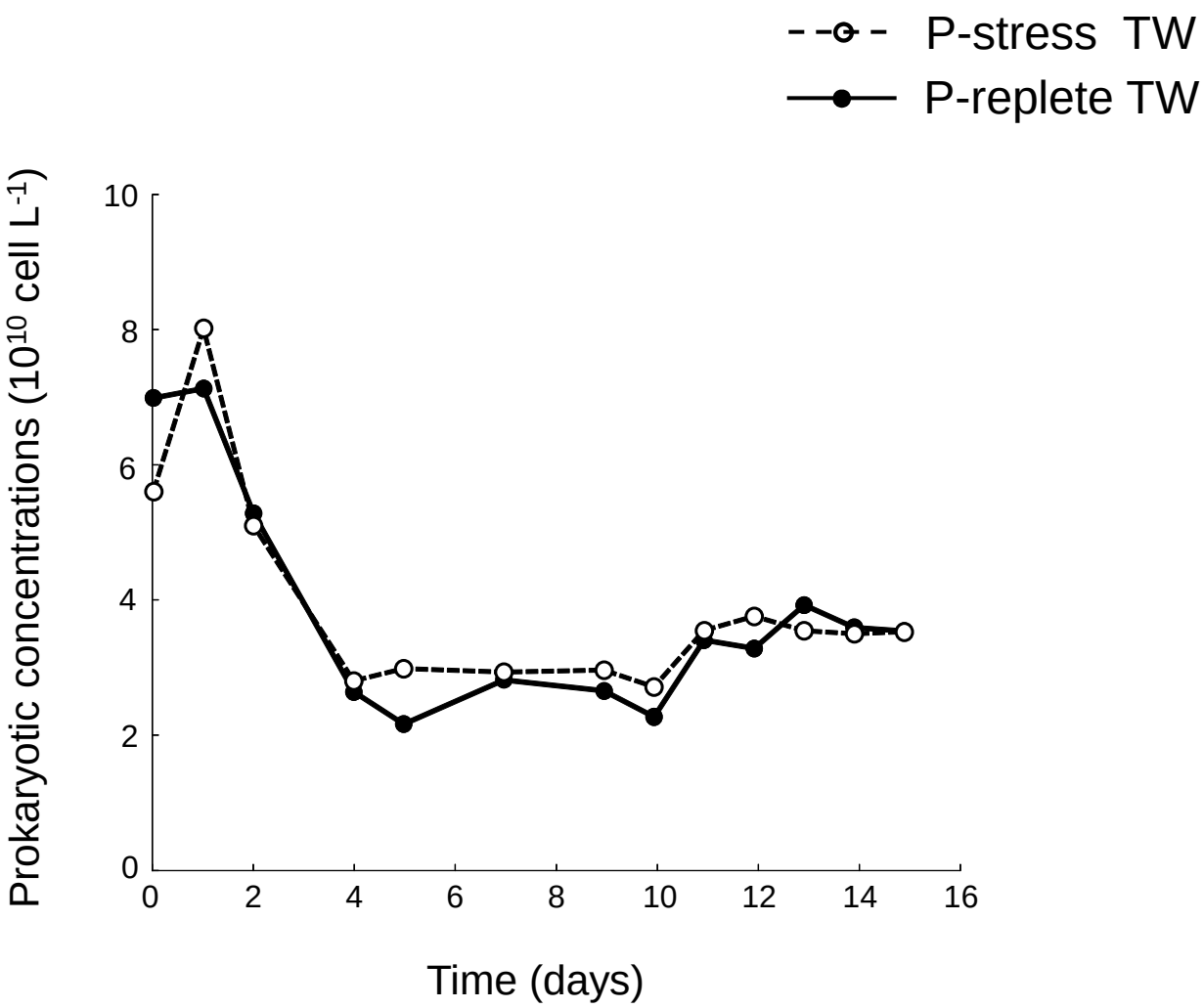
P-stress TW
P-replete TW
Prokaryotic concentrations (10^10 cell L^-1)
10
8
6
4
2
0
0
2
4
6
8
10
12
14
16
Time (days)

Figure 2

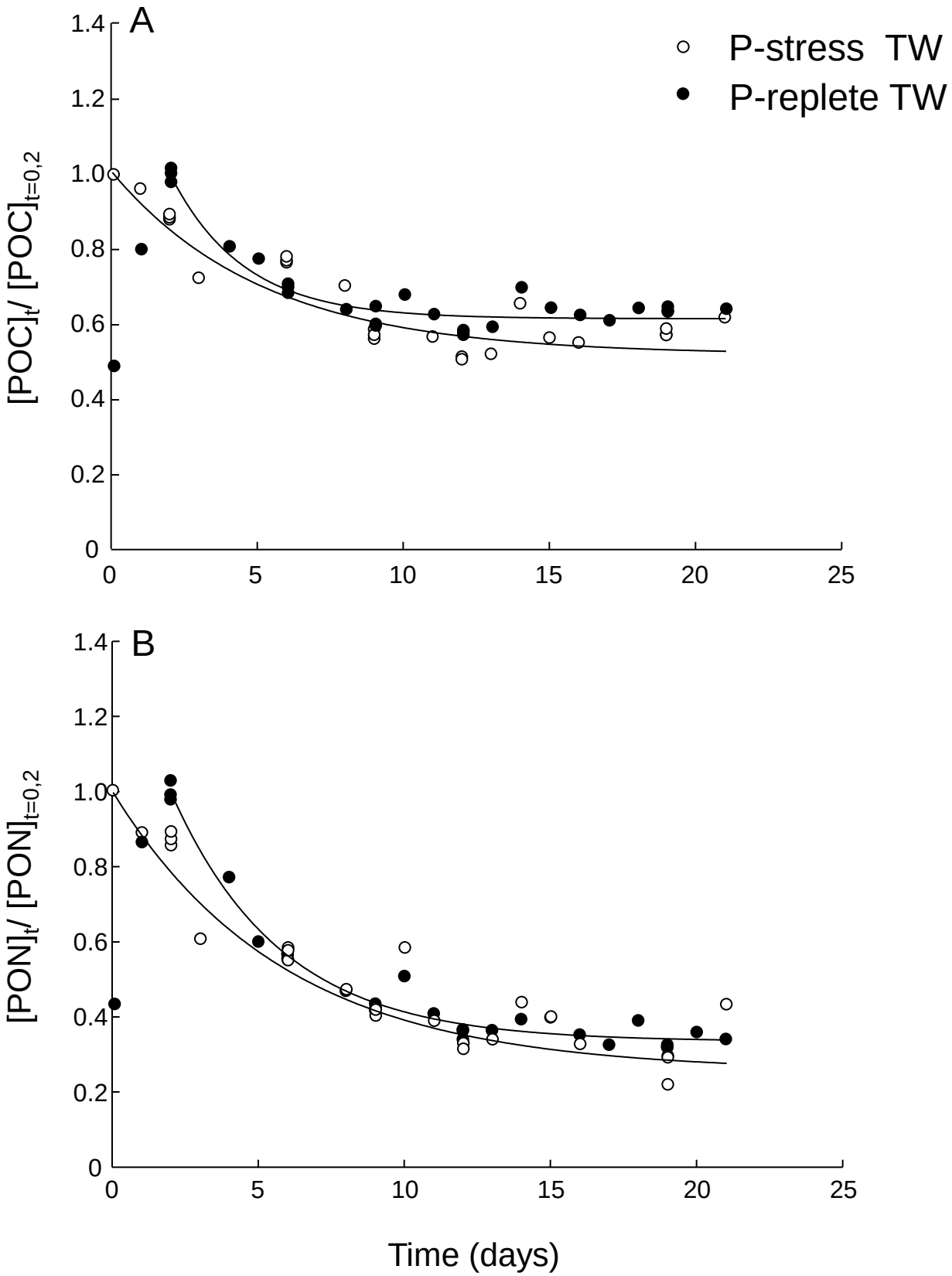
A
P-stress TW
P-replete TW
[POC]t/ [POC]t=0,2
1.4
1.2
1.0
0.8
0.6
0.4
0.2
0
0
5
10
15
20
25
B
[PON]t/ [PON]t=0,2
1.4
1.2
1.0
0.8
0.6
0.4
0.2
0
0
5
10
15
20
25
Time (days)

Figure 3

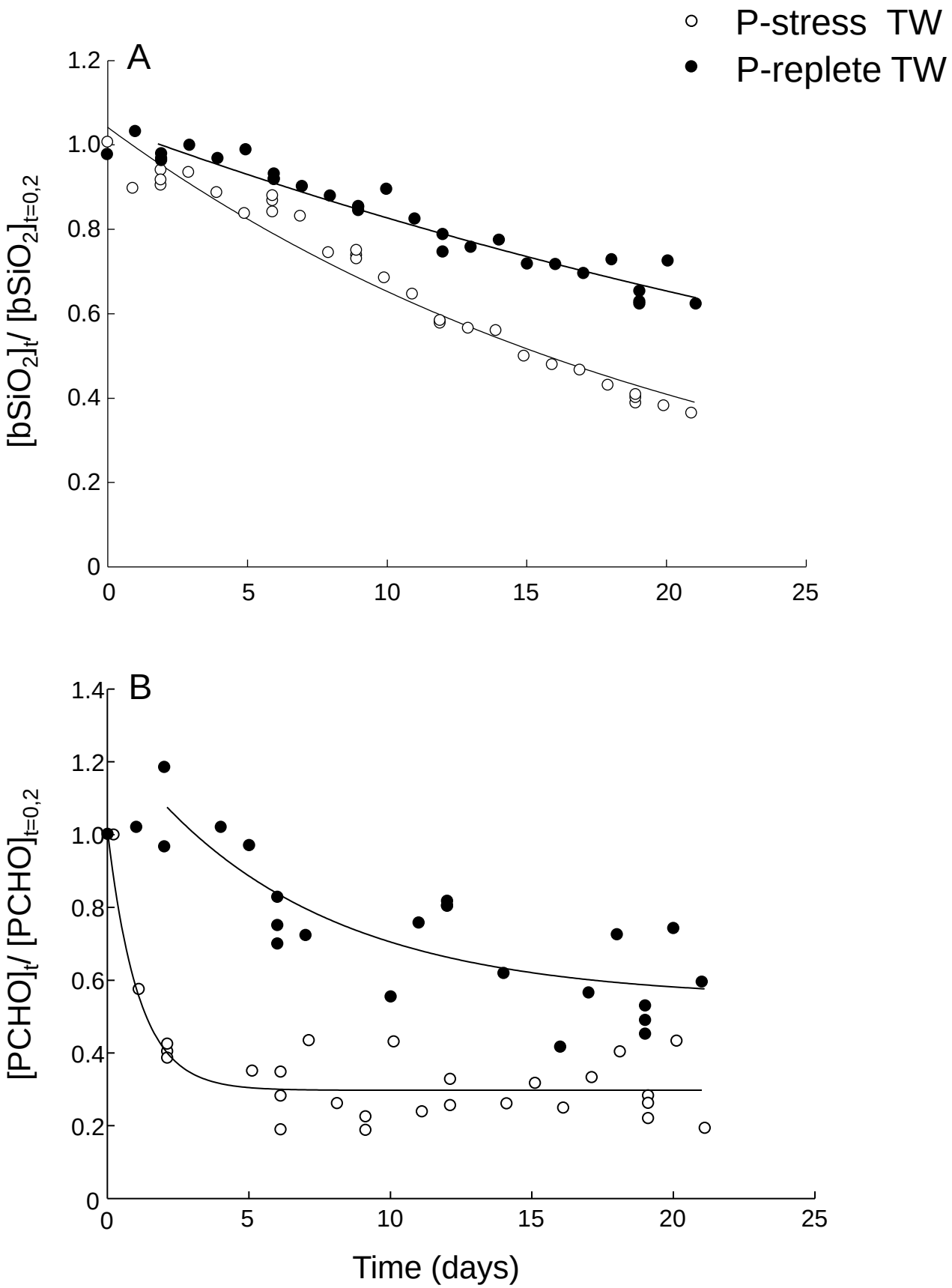
P-stress TW
P-replete TW
A
B
[bSiO2]t/ [bSiO2]t=0,2
[PCHO]t/ [PCHO]t=0,2
Time (days)

Figure 4

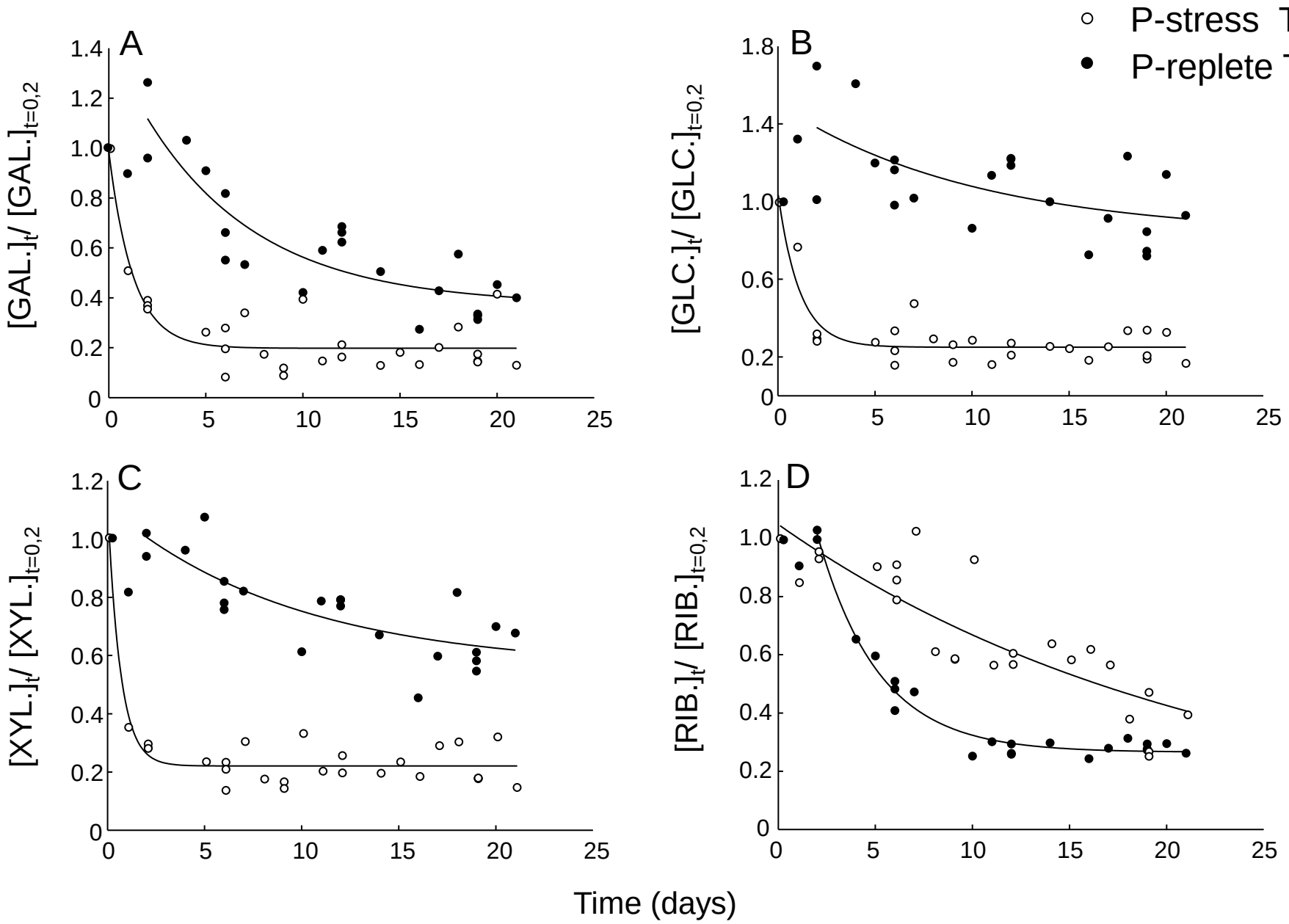
P-stress TW
P-replete TW
A
B
C
D
[GAL.]t/ [GAL.]t=0,2
[GLC.]t/ [GLC.]t=0,2
[XYL.]t/ [XYL.]t=0,2
[RIB.]t/ [RIB.]t=0,2
Time (days)

Figure 5

Supporting information for

Phosphorus limitation affects the molecular composition of *Thalassiosira weissflogii* leading to increased biogenic silica dissolution and high degradation rates of cellular carbohydrates

Christos Panagiotopoulos[1*], Madeleine Goutx[1], Maxime Suroy[1], Brivaela Moriceau[2]

[1]*Aix Marseille Univ., Université de Toulon, CNRS, IRD, Mediterranean Institute of Oceanography (MIO) UM 110, 13288, Marseille, France*

[2]*Université de Brest, Institut Universitaire Européen de la Mer (IUEM), CNRS, Laboratoire des Sciences de l'Environnement Marin, UMR 6539 CNRS/UBO/IFREMER/IRD, 29280 Plouzané, France*

Corresponding author e-mail: christos.panagiotopoulos@mio.osupytheas.fr

Figure legends:

Fig. S1: FTIR spectra of the "P-replete *T. weissflogii*" (black line) and "P-stress *T. weissflogii*" cultures (dash line). Cells analyzed by FTIR come from the preliminary culture experiment that allowed us to establish the culture protocol ensuring a physiological response of *T. weissflogii* cells to P-stress. Cultures preparation: *T. weissflogii* were cultured in duplicate in f/2 and f/2 -free PO_4^{3-} media for 1 week at 18 °C (± 1 °C) under a light/dark cycle (16 h: 8 h) and a photon flux density of 180 µmol photons m^{-2} s^{-1}. Sample preparation: Aliquots of the *T. weissflogii* cultures were centrifuged, frozen and freeze dried. The powder obtained was mixed with potassium bromide (KBr) and milled to obtain a fine powder. The powder was compressed into a thin pellet before being placed in a desiccator (Schott) under 1 bar pressure for 30 minutes. FTIR analysis: spectra were collected on an FTIR spectrometer equipped with a KBr beam splitter and fitted with a deuterated tri–glycinesulfate (DTGS) detector. The figure show spectra between 2000 and 600 cm^{-1} but absorbance spectra were collected between 3600 and 600 at a spectral resolution of 4 cm^{-1} with 10 scans added and averaged. Band assignments: band 1 and 2 are characteristic of amide I (~1650 cm^{-1}) and amide II (~1550 cm^{-1}) functions, respectively, bands 3 to amine, bands 4 are mostly attributed to carbohydrate (Giordano et al. 2001) while the bands noted under 5 in the figure represented the Si–O bounds of the $bSiO_2$ (Coates, 2000; Giordano et al., 2001).

Fig. S2: FTIR spectra of the frustule in the "P-replete *T. weissflogii*" (red line) and in the "P-stress *T. weissflogii*" batch (blue line) at day 2 (T_2) of degradation. Briefly, samples were collected after 2 days of degradation and frustules were extracted according Suroy et al.

(2014). The sample preparation and FTIR analysis were carried out as previously described in the legend of Fig. S1. Band assignments: band 1 (centered around 2850 cm^{-1}) was attributed to lipids (Coates 2000), the bands noted 2 on the spectrum are characteristic of amide I (~1650 cm^{-1}) and amide II (~1550 cm^{-1}) functions (Giordano et al. 2001, Coates 2000), bands 3 are mostly attributed to carbohydrate (Giordano et al. 2001) while the 3 bands noted under 4 in the figure represented the Si–O bounds of the $bSiO_2$ (Coates, 2000; Giordano et al., 2001).

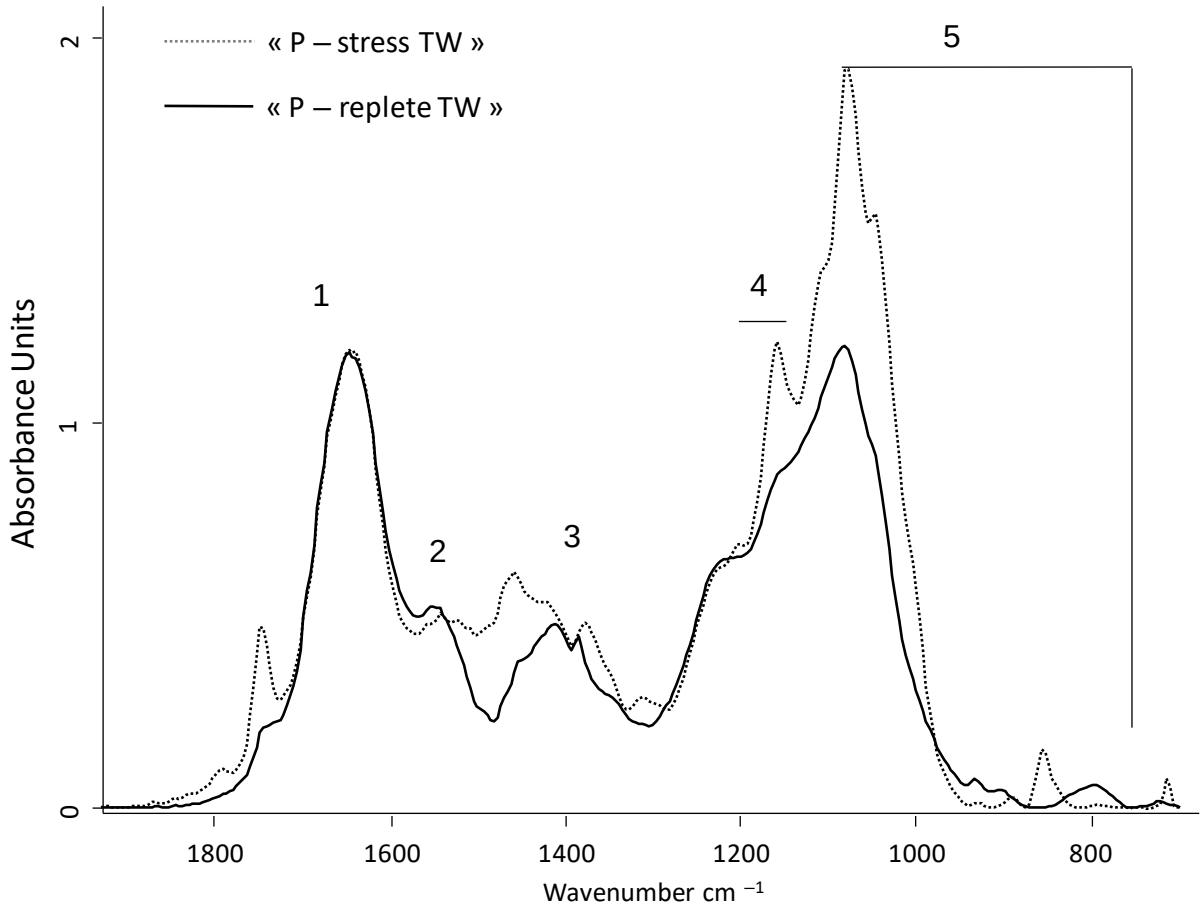

Figure S1

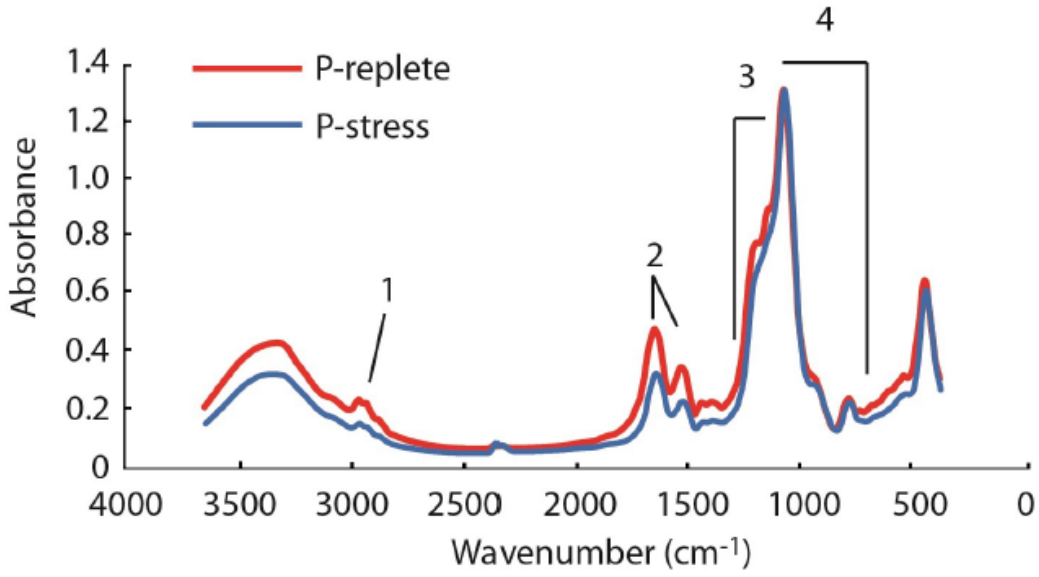

Figure S2

References

Coates, J. (2000). Interpretation of infrared spectra, a practical approach. *Encycl. Anal. Chem.*

Giordano, M., Kansiz, M., Heraud, P., Beardall, J., Wood, B., and McNaughton, D. (2001). Fourier transform infrared spectroscopy as a novel tool to investigate changes in intracellular macromolecular pools in the marine microalga Chaetoceros muellerii (Bacillariophyceae). *J. Phycol.* 37, 271–279.

Suroy, M., Boutorh, J., Moriceau, B. & Goutx, M. 2014. Fatty acids associated to frustule of diatoms and their fate during degradation – a case study in *Thalassiosira weissflogii*. *Deep-Sea Res*. I 86: 21-31.